January 2015

Electromagnetic Band Gap Structure Integrated Wearable Monopole Antenna For Spacesuit

Tahmid Rashid

ELECTROMAGNETIC BAND GAP STRUCTURE INTEGRATED WEARABLE MONOPOLE ANTENNA FOR SPACESUIT

By

Tahmid Rashid

A Thesis
Submitted to the Graduate Faculty

of the

University of North Dakota

In partial fulfillment of the requirements

for the degree of

Master of Science

Grand Forks, North Dakota
December
2015

This thesis, submitted by Tahmid Rashid in partial fulfillment of the requirements for the Degree of Master of Science from the University of North Dakota, has been read by the Faculty Advisory Committee under whom the work has been done, and is hereby approved.

S. Noghanian

Sima Noghanian

Reza Fazel-Rezai

Reza Fazel-Rezai

Isaac Chang

This thesis is being submitted by the appointed advisory committee as having met all of the requirements of the Graduate School at the University of North Dakota and is hereby approved.

Wayne Swisher
Dean of the Graduate School

December 9, 2015
Date

PERMISSION

Title ELECTROMAGNETIC BAND GAP STRUCTURE INTEGRATED WEARABLE MONOPOLE ANTENNA FOR SPACESUIT

Department Electrical Engineering

Degree Masters of Science

In presenting this thesis in partial fulfillment of the requirements for a graduate degree from the University of North Dakota, I agree that the library of this University shall make it freely available for inspection. I further agree that permission for extensive copying for scholarly purposes may be granted by the professor who supervised my thesis work or, in her absence, by the Chairperson of the department or the dean of the Graduate School. It is understood that any copying or publication or other use of this thesis or part thereof for financial gain shall not be allowed without my written permission. It is also understood that due recognition shall be given to me and to the University of North Dakota in any scholarly use which may be made of any material in my thesis.

Tahmid Rashid
DATE: December 2015

TABLE OF CONTENTS

LIST OF FIGURES

LIST OF TABLES

ABBREVIATIONS

ISM	Industrial Scientific and Medical
HIS	High Impedance Surface
CPW	Coplanar Waveguide
SAR	Specific Absorption Rate
FBR	Front to Back Ratio
AMC	Artificial Magnetic Conductor
PEC	Perfect Electric Conductor
PMC	Perfect Magnetic Conductor
CP	Circularly Polarized
HP	Horizontally Polarized
VP	Vertically Polarized
AR	Axial Ratio
EBG	Electromagnetic Band Gap
PBG	Photonic Band Gap
UWB	Ultra-Wide Band
1D	One Dimensional
2D	Two Dimensional
3D	Three Dimensional
UC-HIS	Uniplanar Compact-High Impedance Surface
DTV	Digital Tele Vision
UHF	Ultra-High Frequency
FSS	Frequency Selective Surface
PIFA	Planar Inverted-F Antenna
MIMO	Multiple Input Multiple Output
WLAN	Wireless Local Area Network
GPS	Global Positioning System
PCB	Printed Circuit Board
ICNIRP	International Commission on Non-Ionizing Radiation Protection
GSM	Global System of Mobile
MBAN	Medical Body Area Network
EVA	Extra Vehicular Activity
WBAN	Wireless Body Area Network
PBC	Periodic Boundary Condition
PCB	Printed Circuit Board

ACKNOWLEDGEMENTS

First, I would like to thank my advisor, Dr. Sima Noghanian, for her continuous support, patience, and guidance in completing this research. She always supported me by providing intriguing fundamental thoughts for this research. Without her guidance, I would have never been able to complete this work.

I would also like to thank my committee members, Dr. Reza Fazel-Rezai and Dr. Isaac Chang, for their continuous encouragement and support. They have taught me many things and helped me in overcoming any difficulties I had along the way in this research. Also, I would like to thank Milad Mirzaee and Ala Alemaryeen for their help and motivation.

Additionally, I would like to express my appreciation to North Dakota NASA Experiment Program to Stimulate Competitive Research (ND NASA EPSCoR), and University of North Dakota for the financial support of this project.

Lastly, I would like to thank my family and friends for their love and support.

To my parents,

Harun-ur-Rashid and Jibon Rashid

my sister,

Tamanna Rashid

and my wife

Tasnia Noor

ABSTRACT

Research and development of body-worn communication systems and electronics have become very prominent in recent years. Some applications include intelligent garments equipped with wireless communication devices for sports, astronauts' spacesuits [1], and fire fighters' uniforms [2]. These systems are unthinkable without different kinds of body-worn textile or flexible antennas. In this thesis, we will discuss the design and fabrication of a compact wearable textile antenna within the Industrial, Scientific and Medical (ISM) band operating frequency, proposed for incorporation into a flight jacket of the astronaut inside the habitat. The antenna is integrated with artificial material known as Electromagnetic Band Gap (EBG) structures for performance enhancement. The purpose of the system is to constantly monitor vital signals of the astronauts.

In this thesis the design, simulation, prototype fabrication and antenna testing under different environmental condition, in a word the entire design cycle of wearable Co-Planar Waveguide (CPW) fed monopole antenna is discussed. As human body tissues are lossy in nature, the radiation efficiency of the antenna will be affected due to the absorption of the radiated energy. Therefore, alteration in the radiation characteristics of the wearable antenna like resonant frequency, realized gain and impedance bandwidth will take place. For overcoming these obstacles, addition of EBG layers are recommended to isolate the

antenna from near body environments. The proposed wearable antenna was tested under real operating conditions such as pressure and stretching conditions.

CHAPTER I

INTRODUCTION

The first public research report on wearable antenna goes back to the late nineties [3]. After that the growth in the academic and industrial research on wearable antenna has taken pace and resulted in the design of antennas on flexible substrate followed by textile substrate antennas [4]. The latest embodiments are taking advantages of Electromagnetic Band Gap (EBG) structures for the improvement of antenna performances. In the following section, the motivations behind the research work in this thesis will be highlighted.

1.1 Motivation

Continuous growth of personal communications and handheld devices such as smart phones, organizers, space communication, tablets, computers, navigation devices, etc. which are using wireless access points to transfer data has opened great opportunities in research and development of small antennas and antenna miniaturization techniques. From the engineering point of view the antenna is an indispensable part of any handheld and/or mobile wireless devices. However, for the designers and users, a large piece such as an antenna on the device is inelegant, therefore it is desired to have antennas that are small in size and as much as invisible possible. These demands are reconciled through the development of small antennas, typically integrated into the handheld device's structure.

Antennas' performance are strongly linked with the size and shape of the antennas. The first major results showing the link between antenna size, gain and its maximum bandwidth were presented in the late nineties [18]. The antenna size is not evaluated by the technology used for its fabrication rather by its physical laws. When the size of the antenna is analogous to the wavelength and the antenna is resonating, good performance may be obtained. At usual operating frequencies of wireless networks this means that the antenna should be quite large. Numerous methods and approaches have been experimented and applied to minimize the antenna dimensions as well as maintain good radiation properties.

Immense amount of interest is being shown in the recent years from both academia and industry in the field of flexible electronics. Even more, this research topic is on the top of the pyramid of research priorities requested by many national research organizations. From the market analysis, it is shown that the revenue of flexible electronics is projected to be 30 billion USD in 2017 and over 300 billion USD in 2028 [5].

One specific demand in flexible electronic systems is the requirement of the integration of flexible antennas operating in precise frequency bands as a crucial part of wireless connectivity. This has high demand by today's information oriented society [6]. Obviously, the characteristics of the integrated antenna primarily determine the efficiency of these systems. The flexible wireless technologies require the combination of light-weight, flexible, compact, and low profile antennas. At the same time, these antennas should be efficient, mechanically flexible with a fairly wide bandwidth and desirable radiation characteristics.

Shorted microstrip patches and Planar Inverted F Antennas (PIFAs) are an example of the methods used to reduce the antenna dimensions. To reduce the antenna structure further modifications have to be introduced in the patch. Now-a-days the space filling curves have become popular. Also, many other methods like EBG, metamaterials etc. are being used. The research on antenna designs and performance measurement results presented in this thesis range from gaining experience in the application of miniaturization techniques, material selection to designing antennas and EBG arrays for specific applications in prescribed frequency bands.

1.2 Thesis Outline

Chapter 2 summarizes the significant previous work and ideas that motivate and drive this thesis. The reader will be introduced to the subject of wearable antennas and their applications into different disciplines in the literature review section. The history of wearable antennas and High Impedance Structures (HISs) structures will also be given. Additionally, the relevant theory of EBG will be provided. Their unique electromagnetic properties of in-phase reflection and surface wave suppression will be discussed as well.

In Chapter 3, we will discuss about the Coplanar Waveguide (CPW) fed fully textile monopole antenna. The design parameters, design variables, simulation setup in the CST Microwave Studio [82] are presented. In addition to that the design of the proposed single EBG cell structure and phase reflection characteristic are introduced. The antenna is integrated with EBG for performance enhancement. The simulated as well as measured results of reflection coefficient and radiation patterns are presented.

In order to validate the proposed design for wearable antenna application, performance characteristics of the monopole antenna and the antenna integrated on EBG structure under pressurized and stretching conditions will be discussed in Chapter 4. Stretching in different planes of the antenna structure for different cases, approximating real-life situations, are presented in this chapter.

Chapter 5 is dedicated to discussion of future work and the conclusions of this work. This chapter gives guidelines on how this project can be extended to produce a functional benchmarking tool set.

CHAPTER II

LITERATURE REVIEW

This chapter includes a discussion of the research, challenges and opportunities in the field of wearable antenna and HIS. This includes theoretical background of flexible antenna, and progress involved in developing wearable electronics. It also focuses on the modeling and measurement of environmental effects on the wearable and flexible material.

2.1 Wearable Antenna

2.1.1 Introduction

The aspiration to effortlessly incorporate complete situational consciousness with ever increasing data usage, video, and voice service competencies into body-worn systems has become an area of significant importance, especially for military and emergency first-responder personnel. It has also become severely important and significant to personnel working routinely in the most remote of locations, namely, astronauts.

Wearable antenna has been utilized in many applications, such as in-space applications, military domains, firefighting, personal communications, and health monitoring [7]. They might be a part of a system that provides information about the

wearer's health and environmental states. In general, wearable antennas can be defined as those that can be integrated into clothing.

The requirements can vary depending on the application specifications of wearable antenna. However, some common features that can be listed as follows [8, 9]:

1) Low profile,
2) Flexible and withstand bending, damage from obstacles, and stretching,
3) Low fabrication and maintenance cost,
4) Capable of providing shielding from the adverse effects on the human body,
5) Less disturbing, and not causing extra drag for the operating system, and
6) Hidden and water proof to avoid wet weather conditions.

2.1.2 Wearable Antenna: Types

Textile and fabric-based antenna design is among the overwhelming scrutinize topics in antennas for body-centric communication applications. Generally, wearable antenna necessities those to be low cost, light weight, nearly maintenance-free. A number of occupations need body centric correspondence systems, for example, paramedics, firefighters, and military soldiers. Besides, wearable antennas likewise could make a contribution when connected with youngsters, elders, and athletes for the purpose of monitoring.

The understanding of electromagnetic properties such as permittivity, and loss tangent of the textile material is essential for the design of the textile antennas. Nonconductive textile material like Pellon, silk, felt and fleece may be used as substrates, whereas conductive textile such as pure copper polyester taffeta fabrics, Flectron and Zelt

are some choices suitable for radiating elements. The measurement is done in [10] to find the electromagnetic properties of textile substrate using a transmission/reflection waveguide method.

Depending on the antenna material, wearable antennas can be categorized into two types:

I. Flexible wearable antennas: The antennas that use flexible materials such as foam, polyimides, commercial papers, and flexible Printed Circuit Board (PCB) are called flexible antennas. This type of antennas shows additional flexibility as compared with firm dielectric substrate. The use of this kind is still restricted due to the size of antenna and the complication to be well integrated with clothing in numerous applications. Textile-based antenna is another type of flexible antenna, where the conductive material or/and non-conductive are based on fabrics. Therefore, the integration of the antenna with clothing can be done easily, which can produce more freedom to design without restrictions on the antenna area.

II. Inflexible wearable antenna: The antennas that are made of substrates that are not flexible in nature are called the inflexible wearable antenna. However, these antennas are designed in compact size, made in a curved contoured shape to be mounted on the human body. Regardless of the restrictions on the antenna area and shape, it is impractical and inconvenient to use these kinds of antennas for on-body communication system [11].

2.1.3 Wearable Antennas: Desirable Features and Critical Design Issues

In recent years a lot of attention is being given to wearable antenna due to the fact that they can be integrated into clothing with ease [12, 13-15]. This feature is very much desired for military applications as well, such applications as those requiring low visibility and hands-free. For improving the quality of signal in wireless communications all the available space on clothing can be utilized in wearable antennas.

Another major problem in wireless communication is the drop of signal strength due to multipath fading when the mobile terminal shifts to a wavelength distance. A very efficient way to counter the effect multipath fading is antenna diversity. To utilize the diversity system antenna elements need to be half wavelength apart from each other. Due to lack of space this becomes impractical on small form-factor of hand-held units, which limits the use of antenna diversity. However, in body worn wireless system antenna diversity can be utilized on a large scale [16].

The human body has a frequency dependent permittivity and conductivity with irregularity in shape. Human body geometry, physiological parameters, frequency and polarization of the incident field define the electromagnetic field distribution inside the body and scattering field. As body tissues have high permittivity [17] the resonant frequency of the antenna will change and detune to a lower ones. Antenna gain or the transmitted power in the direction of maximum radiation is another important parameters that are affected due to the conductivity of the human tissues.

Stretching and compression are typical for fabric. The antenna structure can easily deform due to stretching and crumbling and this affects its performance characteristics. As

a result, it will be difficult to mass-produce an antenna with the same radiation characteristics even using the same materials.

Fabric antennas made of textile materials contain voids that can easily absorb water and moisture, and therefore, can change the resonance frequency and impedance bandwidth of an antenna.

In the next section the literature that has contributed to the evolution of wearable antennas will be briefly reviewed and summarized, in order to point out the areas of wearable antenna research that need further study.

2.1.4 Wearable Antennas Literature Review

The research work done on wearable antennas is categorized by the type of antennas used like monopole, dipole, microstrip patch, E-shaped, PIFA and U-slot patch antennas. The applications of the antenna like cellular mobile communications, Frequency Modulation (FM) radio and Television (TV), Global Positioning Systems (GPS), Wireless Local Area Network (WLAN) and Ultra-Wide Band (UWB) wireless systems play a vital role on the categorization of the antenna. Some research that has been done so far on wearable antennas and their applications is summarized below:

A dual band planar antenna was designed for wearable application by Salonen [18] in 1999. It is claimed this antenna was the first of its kind. A U-shaped slot was inserted into a planar inverted F antenna (PIFA) in order to achieve a dual-band antenna for mobile cellular band Global System for Mobile Communications (GSM) 900 MHz band and Industrial, Scientific, and Medical radio (ISM) 2.4 GHz band. The proposed idea was to mount this antenna on the sleeve to make it wearable, although the antenna was made out

of rigid material. The human body effect on the radiation characteristics was minimized by the introduction of the ground plane in the antenna design.

The research on wearable antennas brought noteworthy interest among many researchers in industry and academia. Considering the comfort level of the wearer, a fabric-based wearable antenna for mobile phone antenna for GSM 900 MHz was designed in [19]. Copper plated rip-stop nylon was used to construct the conducting parts and a foam spacer was used as the dielectric. The antenna was placed on the outside of the upper arm in order not to be affected by human, and on-body efficiency was reported to be 50%. In [20] a PIFA wearable antenna which was flexible in nature was designed for 2.4 GHz WLAN and Universal Mobile Telecommunication Systems (UMTS) 2100 MHz. A fleece fabric based microstrip antenna was designed in [3] which is to be used for an emergency workers' outfit at 2.4 GHz WLAN band. The bending effect on wearable microstrip patch antenna was studied in [21]. The study showed that bending in E-plane has changed the resonance frequency, whereas H-plane bending has minimal effects on resonance frequency.

Wearable antennas are gaining popularity in their use in military uniforms [22]. The difficulty is that the radio operators can be easily identified by their protruding antennas and can become targeted by the enemy. In addition, the antennas can be easily broken by trees and bushes, which prohibit their mobility. To overcome these problems different wearable antenna designs seamlessly integrated into a soldier uniform have been proposed [23-25]. As any conducting structure can radiate, if designed properly, some researchers proposed to use the metal button of jackets and belts as antennas [26-28]. The first U-shaped patch antenna design was successfully implemented for wearable applications using copper tape and fleece fabric [14].

As textile-conducting materials continue to find use in wearable antenna designs, it was deemed necessary to characterize their electrical properties. The measurement techniques of surface resistivity and conductivity of electro-textiles were carried out in [29, 30]. The use of electro-textiles in wearable antennas applications was explored in [31]. For this purpose a fabric antenna was designed and its efficiency was reported to be 80%. This research supported the idea of using textile-conducting materials in place of traditional copper for light-weight wearable antennas.

As a result of different textile materials appearing in the area of wearable antenna design, it became necessary to characterize the performance of wearable antenna with different textiles. Testing of six different textile fabrics as wearable antenna substrates is presented in [32]. To achieve uniform separation distance between antenna and textile substrate, it was concluded that the textile material should be inelastic and it should have a smooth surface.

Wearable antennas are meant to work in close proximity to the human body. That is why it is very important to characterize the effect of human body on its performance. The first in-depth research on textile antenna performance close to the human body was given in [33]. The results showed that wearable antennas performed well near human body and performance was only marginally affected by human body interaction.

Major parts of our discussion so far are linearly polarized antennas. In [34] the first circular polarized wearable antenna was presented. A corner-truncated patch was designed for this experiment. To design WLAN wearable antenna with circular polarization another conventional technique of feeding along the diagonal of square patch was employed in

[35]. The intent of these results is to show that conventional antenna design techniques works almost same for textile based antennas. For dual band operation an E-shaped microstrip patch wearable antenna was also proposed [36] using standard designs and results were similar to conventional E-shaped patch design.

A GPS wearable antenna was proposed [37], which uses a water-resistant and fire-resistant foam substrate. This made this antenna especially suitable for using in rescue worker's garments. This antenna was shown to work well even when covered with textiles, integrated into a jacket or worn on the human body. As athletes use very light clothes, to make the wearable antenna feather light a flexible and lightweight antenna at 2.4 GHz was proposed in [38].

Different fabrication techniques of textile antennas were discussed in [39]. For conducting part of the antenna copper tape, copper thread and conductive spray were used to see their effects on wearable antenna performance. It was mentioned that most of the general public will accept wearable antenna if the antennas are hidden, small in size and lightweight.

The large space available on the human body can be used for designing a high gain antenna array. This concept was explored in [40] for a body-worn electro-textile antenna array. A novel wideband antenna element, referred as a complementary-8 element because of its shape, was investigated for use in possible Extra Vehicular Activity (EVA) communication systems. A self-complementary antenna was designed for use above 2.1 GHz, using the Nora conductive fabric and a 0.635-cm Nomex substrate. Investigation of

six complementary-8 antenna elements placed around the periphery of an EVA suit for navigation purposes was discussed in this work.

Federal Communications Commission (FCC) has approved Ultra-wide band (UWB) for different application. UWB is an emerging wireless technology. This technology allows high data rate over short distances with low power consumption [41]. The first UWB textile antenna was proposed in [42] in which, two design topologies were investigated. The first design was a CPW fed disc monopole antenna and the other was a microstrip fed annular slot antenna. The designs had a small thickness of 0.5mm and very flexible to be easily integrated into clothing. A UWB antenna based on a button structure was proposed in [43, 44].

EBG structures are also known as Artificial Magnetic Conductor (AMC) or High Impedance surface (HIS) [45] surfaces. These are getting noticed to be used in antenna designs [46-48] due to their unique electromagnetic properties of in-phase reflection of plane waves and stopband for propagation of surface waves. These properties have been exploited in designing low-profile antennas and improving the bandwidth, gain and backward radiation in patch antenna designs.

The use of EBG structures in wearable antenna designs has not been explored to a great extent, although some designs have been proposed which have incorporated them. The first EBG based antenna design for wearable application was proposed in [49]. Although it was not a truly wearable antenna as it was constructed on traditional rigid FR4 substrate, however the idea was to use this for wearable applications. A 2.45 GHz patch antenna was fabricated on a thin FR4 substrate and EBG pattern was etched on the ground

plane of the antenna. It was observed that the effect of EBG was to increase the impedance bandwidth, and gain, and reduce the backward radiation as well as the size of the antenna.

In [50], the design of flexible M-shaped printed monopole antenna, operating in the ISM 2.45 GHz band, was proposed for telemedicine communications. The antenna substrate was made of polyimide Kapton flexible material, and the AMC ground-plane was used in the design of the antenna in order to isolate the user's body from undesired electromagnetic radiations in addition to minimizing the antenna's impedance mismatch, caused by the high permittivity human tissues. A design of a purely textile patch antenna on top of EBG array, for bandwidth enhancement and size reduction, was presented in [51] for wearable applications. Fleece fabric was used as antenna substrate, and the conducting parts were made of copper tape.

The first truly wearable EBG antenna is presented in [52]. This was a design of a patch antenna fabricated on top of a periodic square patch array, working as EBG. Copper tape was used to make conducting parts of an antenna while the fleece fabric was used as an antenna substrate. The EBG had two effects on the antenna performance. Firstly, it increased the input match bandwidth by 50%, and secondly, it reduced the antenna size for a fixed frequency by 30%. The effect of wearable EBG antenna bending on input match and impedance bandwidth was examined in [53]. It was shown that when the antenna is bent along the direction that determines its resonant length, it has the greatest effect on the input matching and impedance bandwidth.

A dual-band triangular patch antenna integrated with dual-band EBG was proposed in [54]. The dual-band was achieved by a parasitic element close to the triangular patch.

The dual-band EBG was realized by using a combination of patches and concentric rings. It was shown that EBG structure helped in reducing the back radiation by up to 15 dB. In [55] a CPW fed dual band wearable antenna was integrated with a dual band EBG structure. The antenna operated in the 2.45 GHz and 5 GHz WLAN bands. The EBG structure consisted of only 3 x 3 EBG elements, but helped in reducing the backward radiation towards the body by over 10 dB and also improved the antenna gain by 3 dB.

After this extensive review of research work done in the wearable antenna design field the research done on EBG will be highlighted in the next section.

2.2 Electromagnetic Band Gap (EBG) Structures

2.2.1 Introduction

Due to the immense application in commercial and defense industry great attention is given to the research of electromagnetics by the researchers all over the world. The use of microwave started in RADAR systems, and after that it was extensively used in microwave communication systems during World War 2. As a result of this change the demand for more advanced materials in the high frequency performance domain increased and new dimensions in the field of electromagnetic materials opened up.

When the wave has a much smaller period in physical size compared to the wavelength of the electromagnetic wave, different periodic structures such as photonic crystals or EBG structures, have also been termed as “Metamaterial” by some authors. The community of electromagnetic has been fascinated with the research possibilities provided by EBG structures. As a result of the EBG’s attractive electromagnetic properties [56],

these materials have been given immense interest to study for potential applications in antenna engineering.

2.2.2 Classifications of electromagnetic band-gap structures

Defected Ground Structures (DGS):

A Defected Ground Structure (DGS) is located on the ground plane and shaped like an etched lattice. DGS has self-assertive shapes and is situated on the rear metallic ground plane. DGS is realized on the bottom plane with one island placed on both sides of the microstrip line on the upper plane. DGS can be used for the microstrip line by etching defects in the backside metallic ground plane. It has also become a hotspot concepts of microwave circuit design nowadays. Compared to photonic band-gap (PBG) structures, DGS has simple structure and potentially great applicability to design different kinds of microwave circuits, for example amplifiers, filters and oscillators. DGSs have achieved noteworthy interests. It discards specific frequency bands, and consequently it is called electromagnetic band-gap (EBG) structures as appeared in Figure 1 [57]. The DGS cell has a simple geometrical shape, such as a rectangle. Its band-gap and slow-wave characteristics are better than the conventional ground plane. DGSs have picked up very noteworthiness in filter design [58] indicating optimal pass-band and stop-band responses in addition to sharp selectivity and ripple rejection. Application of CPW-based spiral-shaped DGS to Monolithic Microwave Integrated Circuit (MMIC) for reduced phase noise oscillator [57], active devices (Bipolar Junction Transistors (BJTs) and Field-Effect Transistors (FETs) can likewise be mounted utilizing DGS procedure. High amount of isolation is achieved in microstrip diplexer and harmonic control, and can also be achieved in microstrip antenna

structures using DGS. Figure 2 gives the schematic of such a DGS with its approximate surface area. A novel DGS based meander microstrip line providing a broad stop-band is presented in [59]. Novel DGS with Islands (DGSI) is proposed in [58]. Careful selection of the line width guarantees 50Ω characteristic impedance (Z_0).

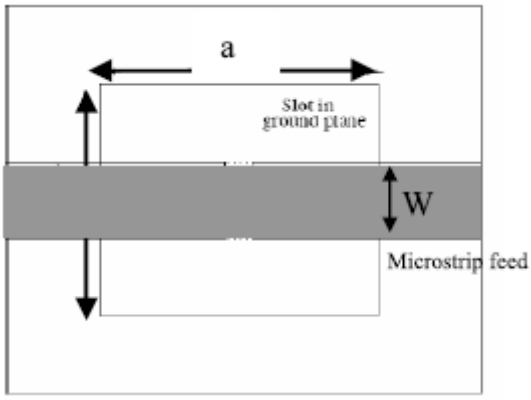

Figure 1: Schematic diagram of a unit DGS cell [4].

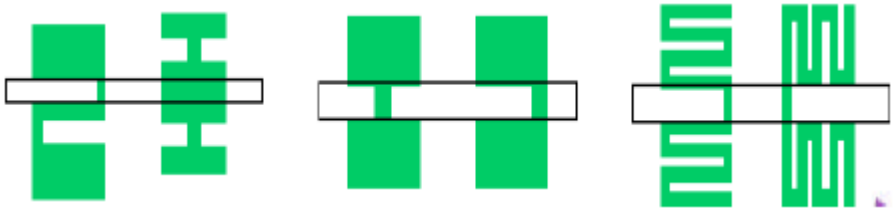

Figure 2: Different shapes of DGS structures [4].

The results from the Electro-Magnetic (EM) simulation of the DGSI and the circuit simulation using extracted parameters are compared [4], showing excellent agreement between the two in a wide band. Examination of stop-band characteristics is studied using concentric circular rings in different configurations. Metallic backing significantly reduces interference effects, harmonics and phase noise. Numerous novel 1D DGS are presented for Microwave Integrated Circuits (MICs), Monolithic MIC (MMICs), Low Temperature Cored Ceramic (LTCC) including Radio Frequency (RF) front-end applications.

Significant changes in the attributes including Slow-Wave Factor (SWF) of intermittent structures like transmission lines is accomplished by means of quite a few unconventional DGS, like spiral-shaped and Vertically Periodic DGS (VPDGS). VPDGSs have been utilized as a part of lessening the dimension of MICs and amplifiers, therefore increasing SWF significantly. Harmonic control can also be achieved in microstrip antenna structures using one-dimensional (1D) DGS [59].

The DGS:

1) disturbs shielding fields on the ground plane,
2) increases effective permittivity,
3) increments effective capacitance and inductance of transmission line,
4) has one-pole Low Pass Filter (LPF) characteristics (3 dB cutoff and resonance frequency), and,
5) provides size reduction for components.

***Photonic Band-Gap (PBG) structures*:**

PBG structures are periodic structures that manipulate electromagnetic radiation in a manner similar to semiconductor devices manipulating electrons. The semiconductor material exhibits an electronic band-gap electrons cannot exist. Similarly, a photonic crystal that contains a photonic band-gap does not allow the propagation of electromagnetic radiation within specific frequencies in the band-gap [60]. This property has a significant importance in many microwave and optical applications to improve their efficiency. The PBG structures were first investigated in [61] by Yablonovitch. Since then, many researchers in various fields, such as physics, electronics, waves, optics, fabrication, and

chemistry, have been engaged in the realization of PBG, localized defect modes, and other microwave and optical properties peculiar to the PBG structures [62]. Some of the common applications in both microwaves and optics are power splitters, switches, directional couplers, high quality filters, and channel drop filters. Figures 3 and 4 show different configurations of PBG structures composed of two different materials. These configurations include 1D, 2D and 3D periodicities. The 2D materials of a PBG structure can be two different dielectric materials or a metal and a dielectric material.

(a) (b) (c)

Figure 3: Examples of different PBG, (a) 1D, (b) 2D and (c) 3D configurations [4].

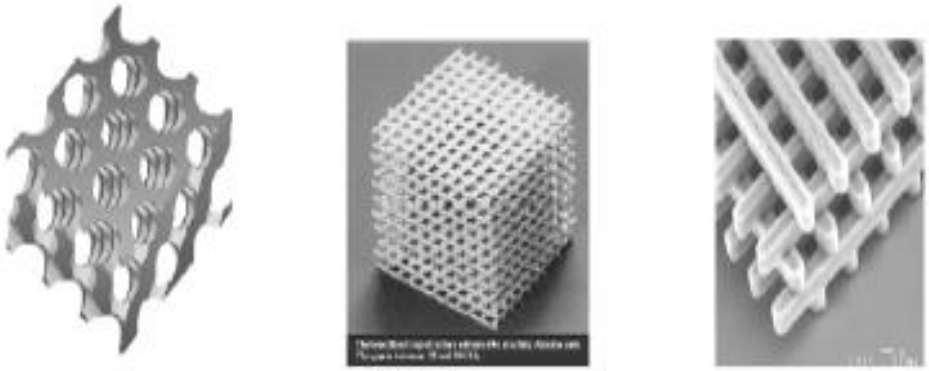

(a) (b) (c)

Figure 4: Typical examples of 3D photonic crystals [4].

The idea of EBG structures starts from the solid-state physics and optic fields. The photonic crystals with forbidden band-gap for light emissions were proposed in [63–64] and after that it was extensively investigated in [65–67]. EBG can be utilized either in 1D, 2D or 3D forms. The directions of the periodicity determine the dimensions. However, 3D EBG are more suitable for getting a complete band-gap because then the waves can be inhibited from all the incident angles. The band-gap in EBG is equivalent to a forbidden energy gap in electronic crystals.

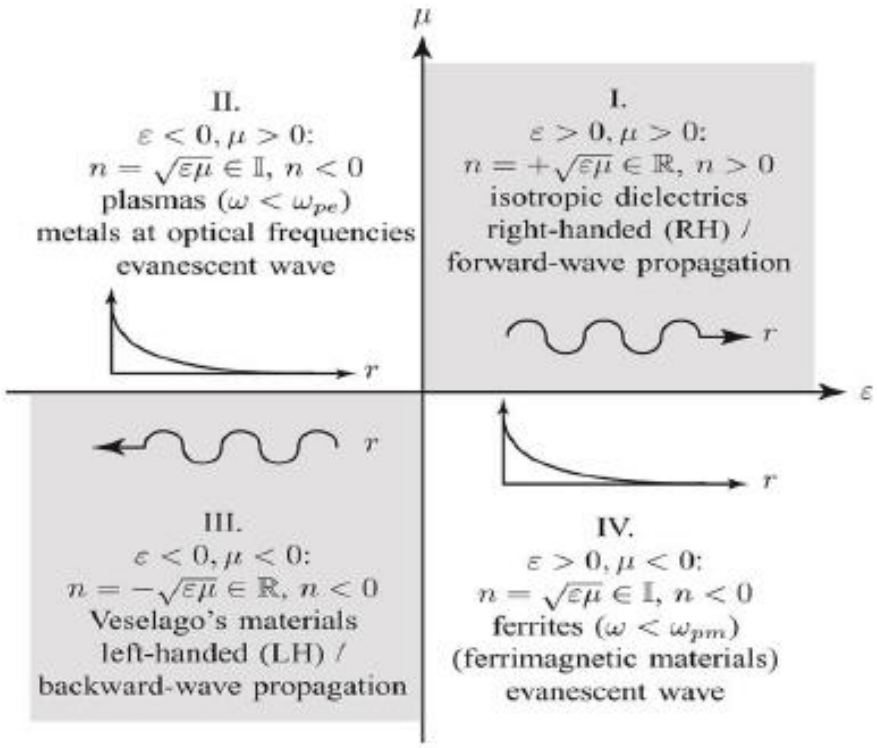

Figure 5: Permittivity, permeability and refractive index diagram [4].

Multiple band-gaps can be created by a periodic structure. Nevertheless, periodicity of the structure is not the only reason behind the band gap in EBG. Individual resonance of one element also plays a vital role. A study showing the mechanisms to form a band-gap in an EBG is presented in [56]. Several applications of EBG are driven by the fact of

the characteristic property of stop-bands at certain frequencies. Within the stop-band the structure acts like a mirror and the electromagnetic wave is completely reflected back. For all other frequencies, structure acts as a transparent medium. Figure 6 illustrates this concept.

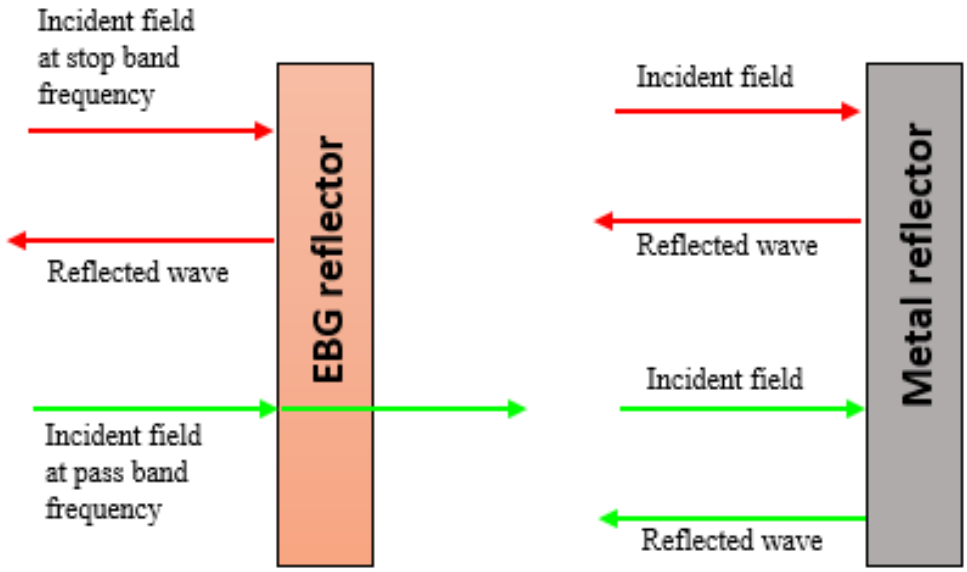

Figure 6: Diagram illustrating the application of EBG as a mirror and its comparison with a metal reflector [63].

If the propagation through the substrate can be prohibited, then the efficiency of the antenna can be increased. This allows the antenna to radiate more towards the main beam direction and as a result it increases the efficiency. The propagation of the electromagnetic waves is effectively prevented within a specific frequency range (the band gap) by these structures. Two illustrations of such geometric structures are given in Figure 7 [69]. As shown in Figure 7, a Metallo-Dielectric (MDEBG) structure is basically a surface that consists of a number of elements. All elements are interconnected with one another to form an array of metallic parts that is embedded in a slab of dielectric.

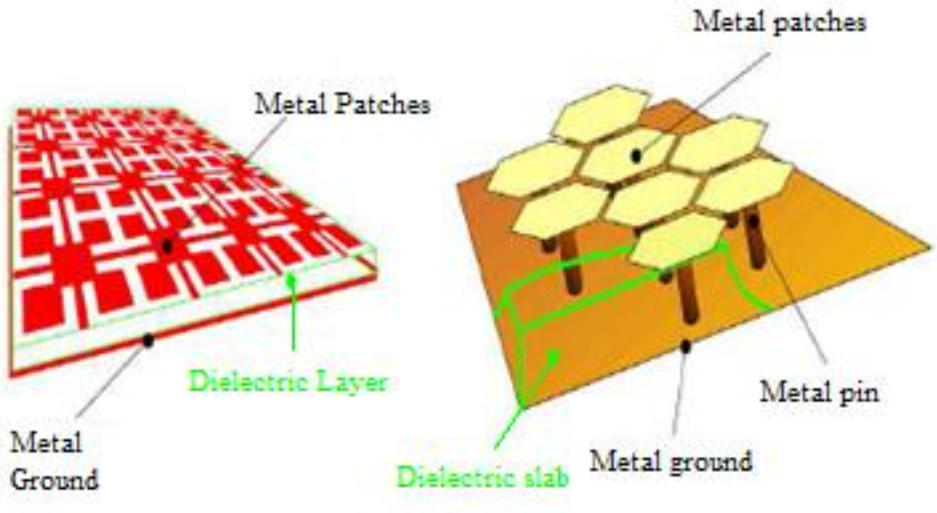

Figure 7: Simple examples of Metallo-Dielectric EBG (MDEBG) structures [4].

2.2.3 Characterization of EBG

2.2.3.1 In-phase Reflection Behavior

Before starting the discussion on in-phase reflection feature of EBG, it is important to present the use of Perfect Electric Conductor (PEC) and Perfect Magnetic Conductor (PMC) as a ground plane in antenna design and their effects on the overall performance of the antenna. In general, the use of the ground plane in the antenna design has two advantages. One, it redirects one half of the radiation into the desired beam, which improves the antenna gain by a factor of 2 or 3 dB, given the correct position of the antenna radiating element; and two, it shields the body underneath the ground plane from the electromagnetic radiation.

While a simple conducting surface has these desirable properties, it also exhibits one undesirable property of inverting the phase of the reflected wave for antenna

applications. As inside a perfect conductor the electric field is zero, the boundary condition of the metal/air interface forces the tangential electric field at the surface to be zero. When an electromagnetic wave is incident on a conductor, the reflected wave undergoes a phase reversal to satisfy boundary conditions of electric field node and magnetic field antinode [70]. Unfortunately, antennas do not operate efficiently if positioned very close and parallel above a PEC ground-plane. By image theory [71] the parallel electric source placed very close above the PEC surface will generate negative image currents on the PEC surface. The image currents in the conductive sheet cancel the currents in the antenna resulting in reduced radiation efficiency. This phenomenon can also be explained by considering the phase shift that occurs as incident wave propagates and then reflects back from the PEC. Finally, it adds to the incident wave and forms an interference pattern on the front side of the radiator. This sequence of operation is shown in Figure 8 for a $\lambda / 4$ distance between the radiator and the PEC ground plane. When an electromagnetic wave travels a distance of $\lambda / 4$ it undergoes a phase change of 90°.

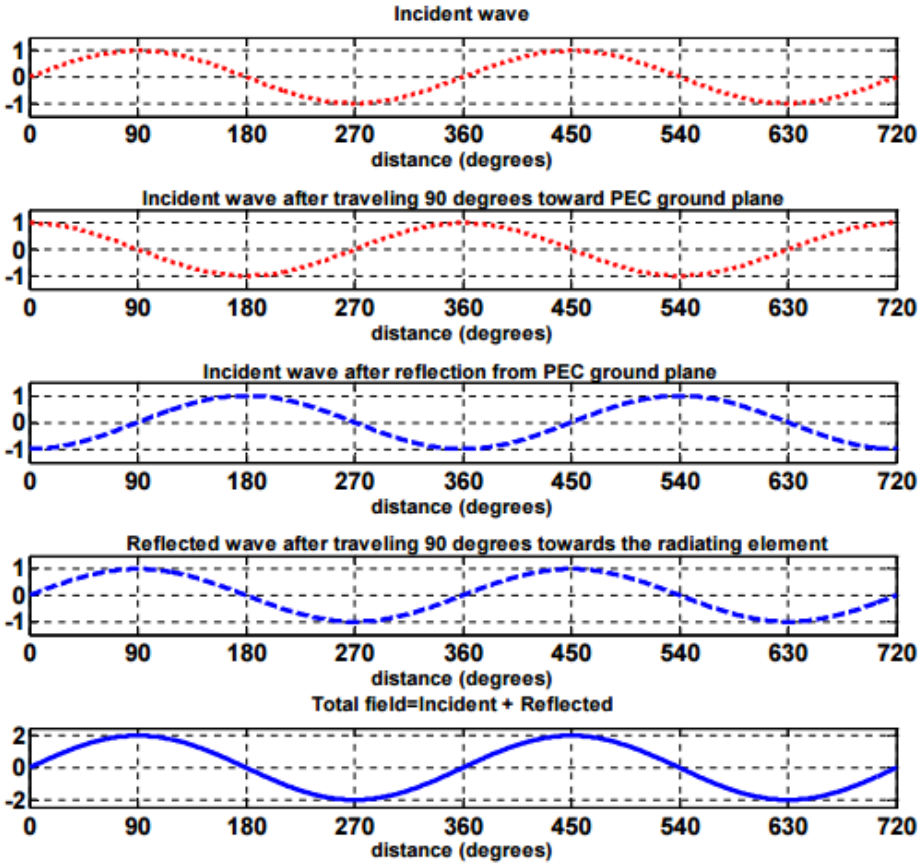

Figure 8: Phase changes of incident wave for a λ/4 spacing between the radiator and PEC ground plane [9].

When wave impinges the PEC ground plane, it is reflected back and undergoes further 180° phase change. It then travels towards the radiator by travelling λ / 4 distance again and in the process its phase changes by a further 90°. Now, as shown in Figure 8, this wave and the incident wave are in phase. They add up constructively in the forward direction. However, if this spacing of λ / 4 is not present, the reflected wave is going to be 180° out of phase, compared to the incident wave, and destructive interference will take place accordingly. This destructive interference phenomenon is shown in Figure 9 for a dipole antenna placed horizontally and very close to a PEC ground plane. The antenna is effectively shorted out by the metal surface and radiation efficiency is reduced significantly

due to destructive interference between reflected waves and original waves emitted directly by the radiating element.

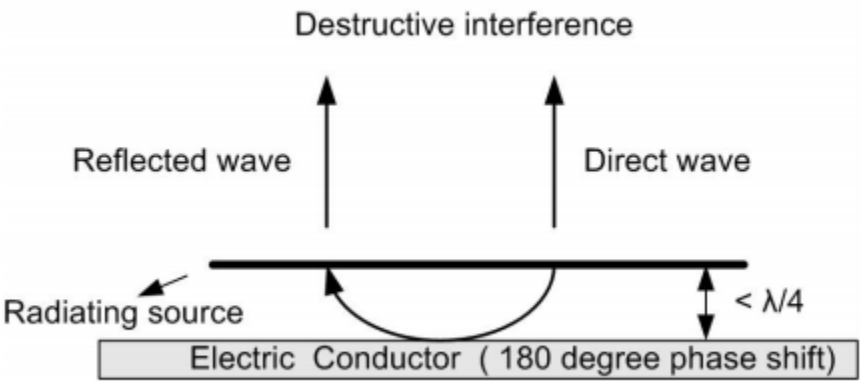

Figure 9: A Radiating element lying parallel and close to electric conductor [9].

This problem can be solved by separating the radiating element from the ground-plane by at least one quarter of the operating wavelength as explained in Figure 8. This situation is depicted in Figure 10, the total phase shift (round trip) from the radiating element, to the conductor surface and back to the element equals one complete cycle. The two waves, therefor, become in phase and will interfere constructively. In this way the antenna will radiate efficiently even when placed close to the electric conductor. However the entire structure requires a minimum thickness of λ/4, which limits its applications in low-profile antenna designs. The low-profile design usually refers to the antenna structure whose overall height at the operating frequency is less than one tenth of a wavelength. Consequently, this minimum thickness requirement is the limitation in reducing the antenna profile, and also in achieving broadband design, as quarter wavelength separation only exists in a certain frequency range.

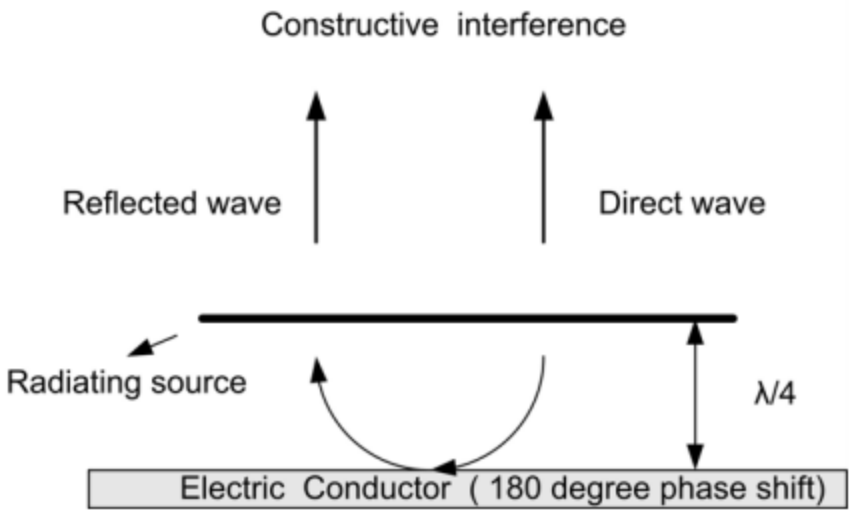

Figure 10: Radiating element separated by ¼ wavelength from the electric conductor [9].

In comparison to a PEC, the Perfect Magnetic Conductor (PMC) will generate in phase image currents, when a horizontal electric source is placed above it. This image current will reinforce the antenna current and increase the radiation efficiency of the antenna. Because the reflected wave has no phase shift upon reflection from PMC surface, the λ / 4 minimum distance is no longer needed. The in-phase reflected waves and the waves radiating directly from the source combine constructively, as shown in Figure 11. This helps to significantly reduce the antenna profile. However, unfortunately no natural material has been found to realize such a magnetic conductive surface.

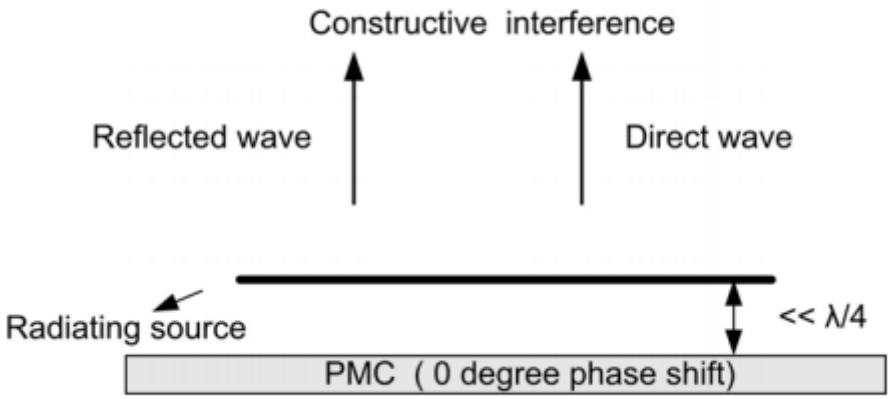

Figure 11: A radiating source lying parallel above PMC ground plane [9].

A significant amount of effort has been devoted to realize a PMC like surfaces artificially. In the next section the artificially engineered HIS or EBG will be discussed that can mimic PMC behavior and has many interesting applications in antenna and microwave field.

However, the reflection phase of an HIS varies from -180° to 180° with frequency. In the range of -90° to 90° of the reflection phase, the reflected wave back from an HIS is more in phase than out of phase with the original radiated wave. This means HIS behaves as PMC at a certain frequency, as shown in Figure 12. HIS showing such characteristics, has been called Artificial Magnetic Conductor (AMC) or Electromagnetic Band-Gap (EBG) structure, and are used as a ground-plane for low profile antenna design [66].

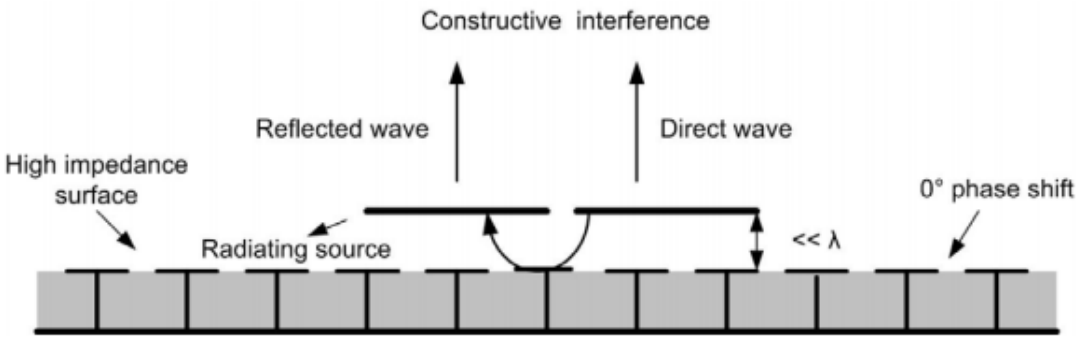

Figure 12: A radiating dipole laying above a HIS ground-plane [9].

In Figure 12 a radiating element laying horizontally above a HIS ground plane is not shorted out as it would on a normal metal ground plane. The HIS ground plane reflects most of the power just like a metal ground plane, however its reflection phase is 0º, unlike 180º of metal sheet, thus allowing the radiating element to be placed directly above the surface. In other words, the image current aid rather than oppose antenna current.

2.2.3.2 Surface wave suppression

A property of conductor surfaces is that they support surface waves [73]. These are propagating electromagnetic waves that are bound to the interface between conductor and free-space. When an antenna operates close to a conductive sheet, it will radiate plane-waves into free space; however, it will also induce surface currents that will propagate along the conducting sheet. If the conductor is smooth and infinite in extent, the surface currents will not radiate into free-space and would result only as a slight reduction in radiation efficiency. In a real situation, the conducting ground-plane is always finite in size and not perfectly smooth. So these surface currents will propagate until they reach a discontinuity like an edge or corner. They will radiate and interfere with the antenna

radiation. The combined radiation from the antenna and different parts of the conducting ground- plane will form a series of lobes and nulls at various angles that will be seen as ripples in the far-field radiation pattern [74]. In addition parts of the surface currents will also radiate on the back side of the ground plane, decreasing front-to-back ratio. Moreover, when multiple antennas share the same ground-plane to form an array, surface currents in addition to free-space coupling also cause unwanted mutual coupling among them [75]. This may cause scan blindness in phased arrays [76]. In reality, due to the finite size of the ground plane, the surface waves can propagate until they reach the dielectric to the air boundary and then radiate into free-space in a cylindrical fashion, which causes a kind of multipath interference with the space waves, as illustrated in Figures 13 and 14.

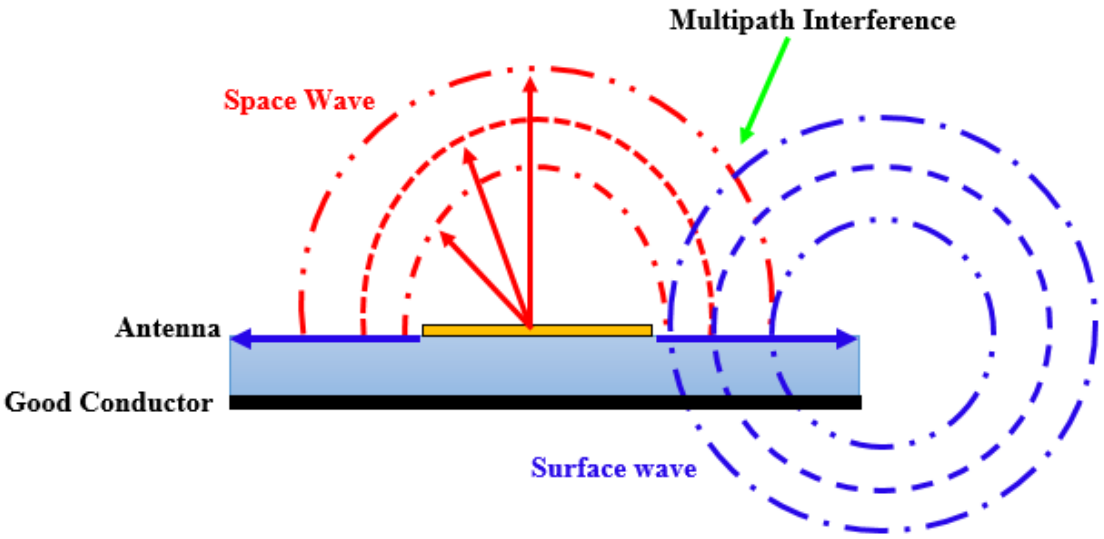

Figure 13: Multipath interference due to the surface waves on normal ground plane [4].

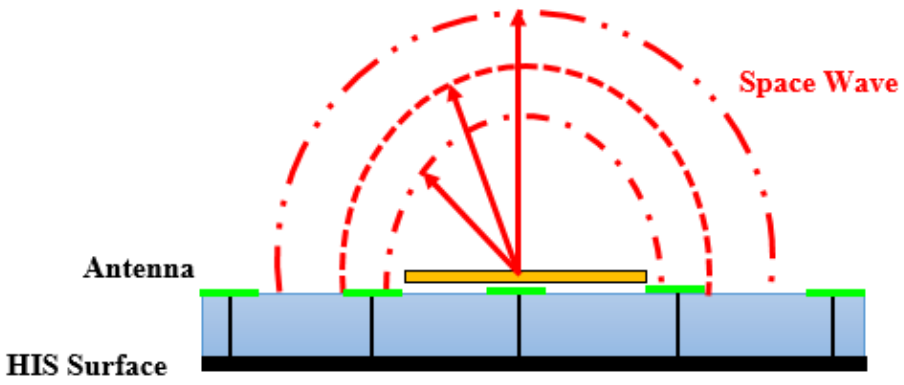

Figure 14: Multipath interference due to the surface waves on alternative ground plane with HIS structure [4].

Surface wave suppression property is exploited to enhance printed antenna performance. The boundary between two different materials such as air and metal usually gives rise to the surface waves. They are bound to the interface and attenuate exponentially in the direction normal to the interface. The fields associated with surface waves usually extend thousands of wavelengths into the surrounding space at radio frequency and are frequently depicted as surface currents [72]. Surface waves exist mostly because of the finite size of the antenna ground plane. They reduce antenna gain, efficiency and bandwidth. By integrating HIS structure as a ground-plane with printed antennas, surface waves cannot propagate due to band-gap behavior. The increased amount of power couples to the space waves. Thus, antenna placed on HIS ground plane shows much improved radiation pattern performance as compared to those on a normal PEC ground plane.

The unwanted effects of surface waves are expeditiously suppressed in many antenna designs, using EBG structures. EBG structures have been successfully utilized to improve the radiation pattern in the forward direction, reduce backward radiation and,

hence, increase in the gain, and improve the Front-to-Back-Ratio (FBR). For example, the integration of EBG structures with microstrip antenna arrays has been explored to reduce the mutual coupling between elements. In [77], a double layer EBG structure has been used for broadband mutual coupling reduction between UWB monopoles.

It is worth mentioning that there are some structures, which show both EBG and AMC characteristics. For example, the mushroom-like HIS [45] and the uni-planar HIS [78] belong to both groups. Initially, it was proposed that if there were no vias in the mushroom like HIS, it does not show EBG behavior [79]. However, in [80], it was experimentally proved that when via is removed from the mushroom-like HIS, the EBG phenomenon still exists, but the spectral position moves to the higher frequency band, while the AMC band remains at the same position as in mushroom-like HIS. It was then proposed that by varying the periodicity of the HIS structure and keeping the patch size fixed, the AMC and EBG bands can be tailored independently and designed to overlap for simultaneous EBG and AMC operation.

2.2.4 Design of single patch antennas with EBG

The conventional half-wavelength size is relatively large in modern portable communication devices. Various techniques have been proposed, for example, cutting slots, using shorting pins, and designing meandering microstrip lines. Increasing the dielectric constant of the substrate is also a simple and effective way in reducing the antenna size. Compact size and conformability can be achieved for Microstrip Patch Antennas (MPAs) on a high dielectric constant substrate, which make its application a growing interest. Due to the result of strong surface waves excited in the substrate, quite a

few drawbacks are there with the use of high dielectric constant substrate, namely, narrow bandwidth, low radiation efficiency, and poor radiation patterns. If we increase the thickness of the substrate it will help expand the frequency bandwidth, however, stronger surface waves will be there as a result. Consequently, the radiation efficiency and patterns of the antenna are further degraded. To quantify this phenomenon, a comparative study of MPAs on substrates with different dielectric constants and different thicknesses is performed in [4]. Table 1 illustrates the four samples under study. Two of them with low dielectric constant substrate ($\varepsilon_r = 2.2$) and the other two are built on the high dielectric constant substrate ($\varepsilon_r = 10.2$).

Table 1: The patch antenna parameters [4]

Example	Patch size mm^2	Dielectric Constant (ε_r)	Height
1	18 × 10	2.2	1
2	16 × 13	2.2	2
3	9 × 6	10.2	1
4	8 × 6	10.2	2

The simulated S_{11} of the four structures is shown in Figure 15. By tuning the feeding probe location and patch size, all the antennas match well to 50 Ω around 5.1 GHz. It is noticed that the patch sizes on the high dielectric constant substrate are remarkably smaller than those on the low dielectric constant substrate as shown in table 5, which is the main advantage of using high dielectric constant substrate. However, the antenna bandwidth (S_{11} < -10 dB) on 1 mm substrate height is decreased from 1.38% to 0.61% when the ε_r is increased from 2.2 to 10.2. A Similar phenomenon is observed for 2 mm height, the bandwidth is decreased from 2.40% to 1.71%. For the same dielectric constant substrates,

the antenna bandwidth is enhanced when the thickness is doubled. For example, the antenna bandwidth on the high dielectric constant substrate is increased from 0.61% to 1.71% when the substrate thickness is increased from 1 mm to 2 mm. It's important to point out that the bandwidth of example (4) is even larger than that of example (1), which means that the bandwidth of MPAs on high permittivity substrates can be recovered by increasing the substrate thickness.

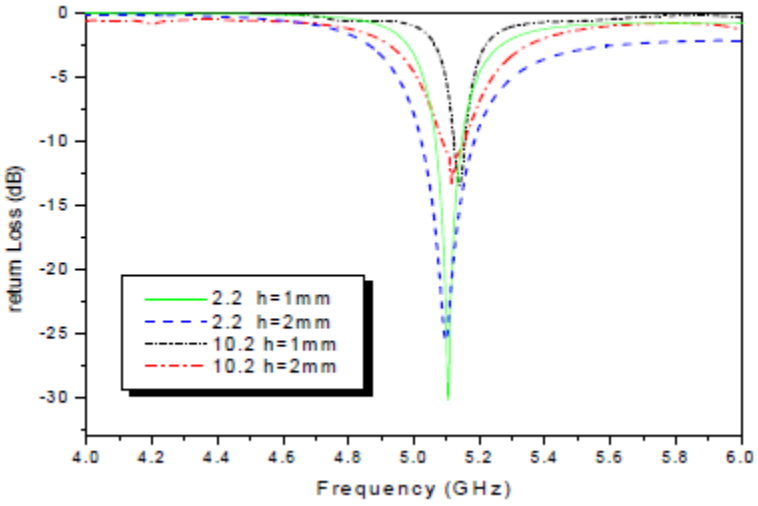

Figure 15: Reflection coefficient comparison of patch antennas with different dielectric constants and substrate height [4].

Figure 16 compares the H-plane radiation patterns of these four antennas. A finite ground plane of λ × λ size is used in the simulations, where λ is the free space wavelength at 5.1 GHz. The antennas on the high dielectric constant substrates exhibit lower directivities and higher back radiation lobes than those on the low dielectric substrates. For antennas on the same dielectric constant substrate, when the thickness increases, the antenna directivity decreases, especially for those on high dielectric constant substrates.

Similar observations are also found in the E-plane patterns. These phenomena can be explained from the excitation of surface waves in the substrate. When a high dielectric constant and thick substrate is used, strong surface waves are excited. This causes reduction of the radiation efficiency and directivity. In addition, when the surface waves diffract at the edges of the ground plane, the back radiation is typically increased.

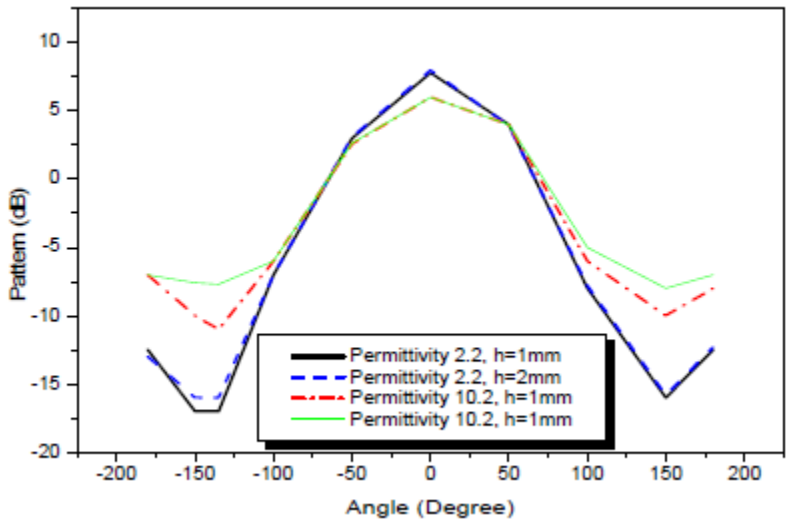

Figure 16: H-Plane radiation pattern of patch antennas with different dielectric constants and substrate heights [4].

2.2.4.1 Gain enhancement of a single patch antenna

Different methods are suggested to overcome the disadvantages of using the thick and high dielectric constant substrate, for manipulating the antenna substrate. One approach suggested is to lower the effective dielectric constant of the substrate under the patch using micromachining techniques [81]. Larger patch size than that on an unperturbed substrate is a shortcoming of this approach. Alternatively, synthesized low dielectric constant substrate or band gap structure can be used to surround the patch so that the surface

waves' impacts can be reduced. An MPA design is proposed that does not excite surface waves [4]. To overcome the unwanted features of the high dielectric constant substrates EBG structure is applied in patch antenna design while maintaining the desirable features of utilizing small antenna size.

2.2.4.2 Patch antenna surrounded by EBG structures

An MPA surrounded by a mushroom-like EBG [4] structure is shown in Figure 17. The surface wave band gap of the EBG is designed in such a way so that it covers the antenna resonance frequency. Thus, the EBG structures constrain the propagation of the surface waves excited by the patch antenna. To effectively suppress the surface waves, four rows of EBG cells are used in the design. It can be noted that the EBG cell is very compact because of the high dielectric constant and the thick substrate employed. As a result, the size of the ground plane can remain small, for instance $1\lambda \times 1\lambda$. MPA designed on a step-like substrate is also investigated due to comparison. By using a thick substrate under the patch the antenna bandwidth can be kept and by using a thin substrate around the patch the surface waves can be reduced. The distance between the patch and the step needs to be chosen carefully. If the distance is too small, the resonance frequency of the patch will change and the bandwidth will decrease. However, when the distance is too large, it cannot reduce the surface waves effectively. To validate the above design concepts, four antennas were simulated on RT/Duroid 6010 ($\varepsilon_r = 10.2$) substrate with a finite ground plane of 52×52 mm^2. Two of them are normal patch antennas built on 1.27 mm and 2.54 mm thick substrates as references. The step-like structure stacks two 1.27 mm thick substrates under the patch and the distance from the patch edge to the step is 10 mm. The EBG structure is built on 2.54 mm height substrate and the EBG patch size is 2.5×2.5 mm^2 with 0.5 mm

separation. Figure 18 compares the measured S_{11} results of these four antennas. All the four patches are tuned to resonate at the same frequency 5.1 GHz. It is noticed that the patch on the thin substrate has the narrowest bandwidth of only 1% while the other three have similar bandwidths of about 3–4 %. Thus, the thickness of the substrate under the patch is the main factor determining the impedance bandwidth of the antenna. The step substrate and the EBG structure, which are located away from the patch antenna, have less effect on the antenna bandwidth.

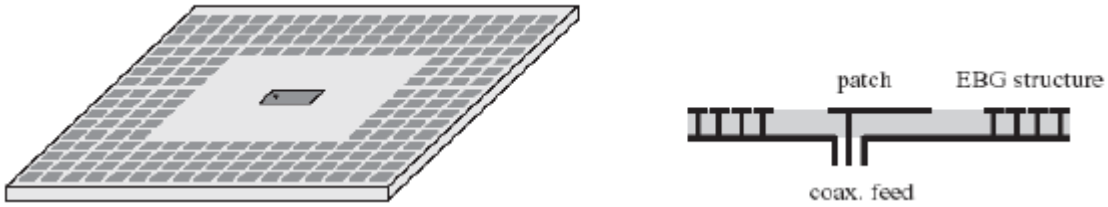

Figure 17: Patch antenna surrounded by a mushroom-like EBG structure: (a) geometry and (b) cross section [4].

The antenna on the height 2.5mm has the lowest front radiation while its back radiation is the largest. When the substrate thickness is reduced, the surface waves become weaker and the radiation pattern improves. The step-like structure exhibits similar radiation performance as the antenna on the thin substrate. The best radiation performance is achieved by the EBG antenna structure. Due to successful suppression of surface waves, its front radiation is the highest, which is about 3.2 dB higher than the thick case. Since the surface wave diffraction at the edges of the ground plane is suppressed, the EBG antenna has a very low back lobe, which is more than 10 dB lower than other cases. Table 2 lists the simulated results of these antennas. Note that the radiation patterns are normalized to the maximum value of the EBG antenna.

Table 2: Simulated performance of four different MPA designs on the high dielectric constant substrate.

Antenna	Bandwidth %	Front Radiation	Back Radiation
Thin	1	-2.3	-15.5
Thick	4	-3.2	-12
Step stair	4.7	-2	-14
EBG	3	0	-25

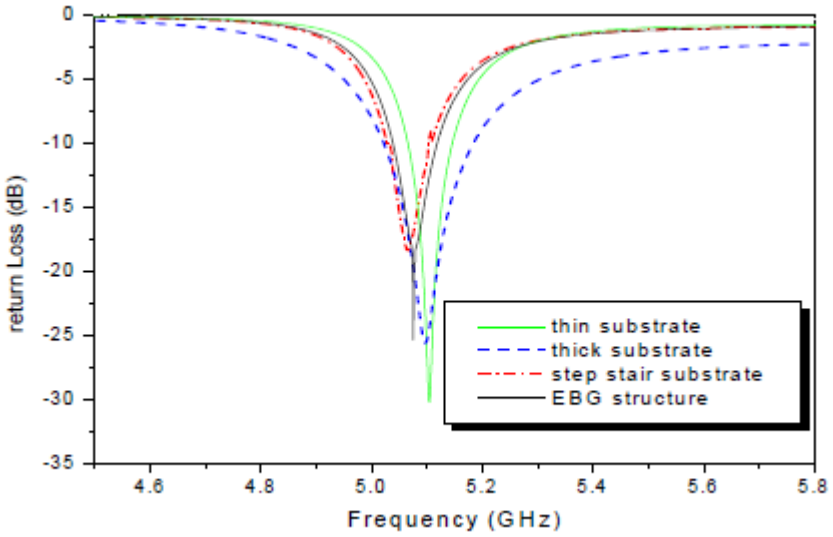

Figure 18: Comparison of the measured reflection coefficient of the four MPA structures [4].

It is also interesting to notice that in the E-plane the beam-width of the EBG case is much narrower than the other three cases whereas in the H-plane it is similar to other designs. The reason is that the surface waves are mainly propagating along the E-plane as shown in Figure 19. Once the EBG structure stops the surface wave propagation, the beam becomes much narrower in the E-plane. From above comparisons it is clear that the EBG structure improves the radiation performances of the patch antenna while maintaining its compact size and adequate bandwidth.

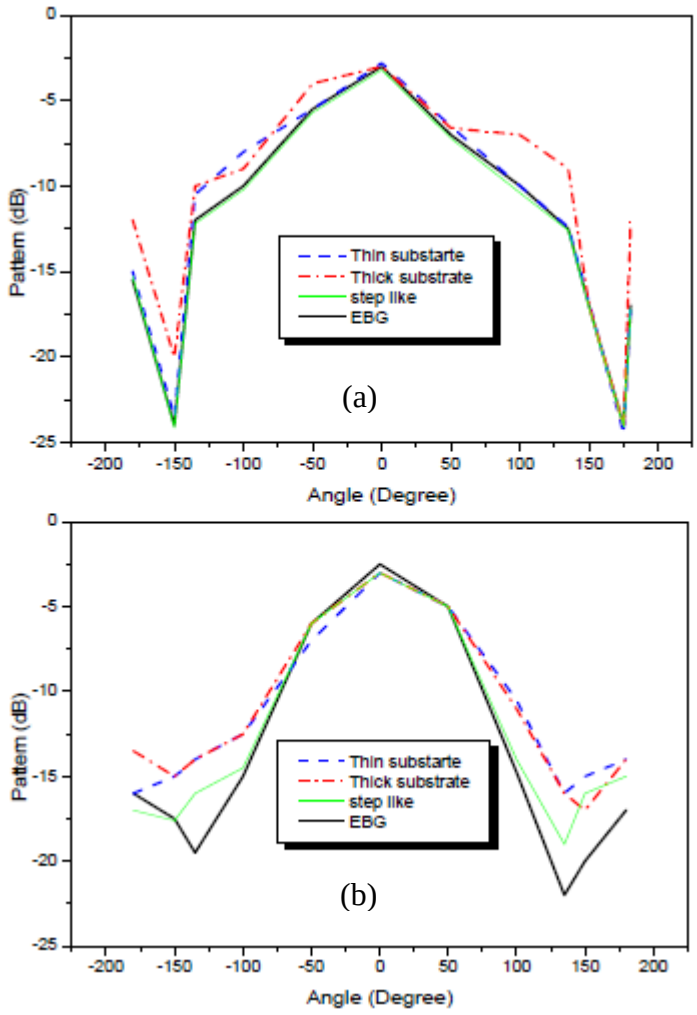

Figure 19: Simulated radiation patterns of different patch antennas: (a) E-plane and (b) H-plane pattern [4].

CHAPTER III

TEXTILE MONPOLE ANTENNA INTGRATED WITH EBG

In this chapter, the design cycle of the CPW fed textile monopole antenna and flexible EBG structure, simulation and measurement results will be presented. The antenna key performance indicators such as reflection coefficient (S_{11}), impedance bandwidth, antenna gain, co-polarization and cross-polarization are studied and compared for the monopole antenna with and without EBG reflector.

3.1 Introduction

3.1.1 Reflection Co-efficient (S_{11})

A parameter that describes the amount of an electromagnetic wave that is reflected back by the discontinuity of an impedance in the transmission medium is called reflection coefficient. S-parameters describe the input-output relationship between ports (or terminals) in an electrical system. If we have two ports we call them port 1 and port 2. Here, S_{12} will symbolize the power that is transferred from port 2 to port 1. On the other hand, S_{21} will represent the power transferred from port 1 to port 2. In summary, S_{nm} denotes the power transferred from port *m* to port *n* in a multi-port network.

S_{11} is the most commonly quoted parameter in regards to antenna design, since a single antenna element is a one-port system. S_{11} represents the amount of power that is reflected from the antenna, and therefore it is also known as the reflection coefficient (also known as gamma = Γ or return loss). If S_{11}=0 dB the power that is supplied to the antenna is reflected back from the antenna and as a result nothing is radiated. If S_{11}= -10 dB, this indicates that 10% of the power that is delivered to the antenna is reflected. The remaining 90% of power is delivered or accepted by the antenna. This amount of power is either radiated by the antenna or absorbed as losses within the antenna. As antennas are usually designed to be low loss, most of the power delivered to the antenna is radiated.

3.1.2 Realized Gain

Compared to that of an isotropic source the power that is transmitted in a specified frequency in a particular direction (usually in the direction of signal propagation) is called antenna's realized gain. As antenna gain takes into account the real losses that occur, generally gain is mentioned in the antenna's specification sheet. Gain is the key performance figure and is a product of the antenna's electrical efficiency and directivity. From a transmitting antenna perspective, the gain parameter defines how efficiently the antenna converts the input power into radio waves in a specified direction. From the perception of a receiving antenna, the same gain parameter describes how efficiently the antenna converts radio waves into electrical power. An antenna that has a gain of 3 dBi means that the received power from the antenna in the far-field will be 3 dB higher (twice as much) compared to that of the amount of power a lossless isotropic antenna would receive with the same input power.

The realized gain is determined by the antenna shape, the material, input impedance matching, and the antenna's surrounding environment. Radiation patterns characterize the variation of the radiated far-field intensity of an antenna as an angular function at a specific frequency. Usually, they are shown as cuts along two orthogonal planes of the antenna, namely E-plane and H-plane. In this thesis the antenna is placed on XY plane and facing towards +Z direction, so the radiation patterns are defined in the same manner for all antennas investigations, so that, E-plane is YZ plane and H-plane is XZ plane. Also, these planes can be defined by the cut angle, so that, E-plane is defined at $\varphi=90°$ and H-plane is defined at $\varphi=0°$, where φ is the angle measured from x axis.

3.1.3 Co- and Cross-Polarization

Co-polarization (co-pol) is the polarization that is in the direction of the desired polarization. On the other hand, cross-polarization (X-pol) is the polarization that is orthogonal to the polarization being discussed. For example, if the antenna is designed in a way that the fields are meant to be horizontally polarized, then the cross-polarization happens in vertical direction and co-polarization happens in horizontal direction. In the case of circular polarization with Right Hand Circularly Polarized (RHCP), then co-polarization is RHCP and the cross-polarization is Left Hand Circularly Polarized (LHCP). These terms appear because an antenna is never 100% polarized in a single mode polarization (linear, circular, etc.). Therefore, two radiation patterns of an antenna are presented sometimes, the co-pol (or desired polarization component) radiation pattern and the cross-polarization radiation pattern.

3.2 Design Characteristics and Performance Results of the Proposed CPW-Fed Textile Monopole Antenna

The CPW-fed monopole antenna is designed to operate in IEEE 802.11 frequency band of 5.725-5.875 GHz band (ISM band). This frequency band is used in space biomedical application, earth stations, microwave links and Radar and, amateur radio. The antenna is designed, simulated and optimized using commercial electromagnetic simulation software CST Microwave Studio [82]. The radiating element of the antenna is square shaped with two slots. The feeding method is through a CPW feeding line. This feeding method helps the antenna to be uniplanar, which can eliminate the problems associated with the alignment of different conducting layers. Pellon, which is a textile material with a thickness of 1.8 mm, relative dielectric permittivity (ε_r) of 1.08 and electrical loss tangent of 0.008 is used as a substrate material for the antenna. Two layers of the substrate made the antenna height 3.6 mm. Figure 20 (a) and Table 3 show the design and parameters of the antenna. Pellon fabric is chosen as the antenna's substrate since it exhibits a low profile and flexible characteristics, also the thickness can be controlled by stacking up multiple layers. The conducting material of the antenna is nickel/copper ripstop fabric.

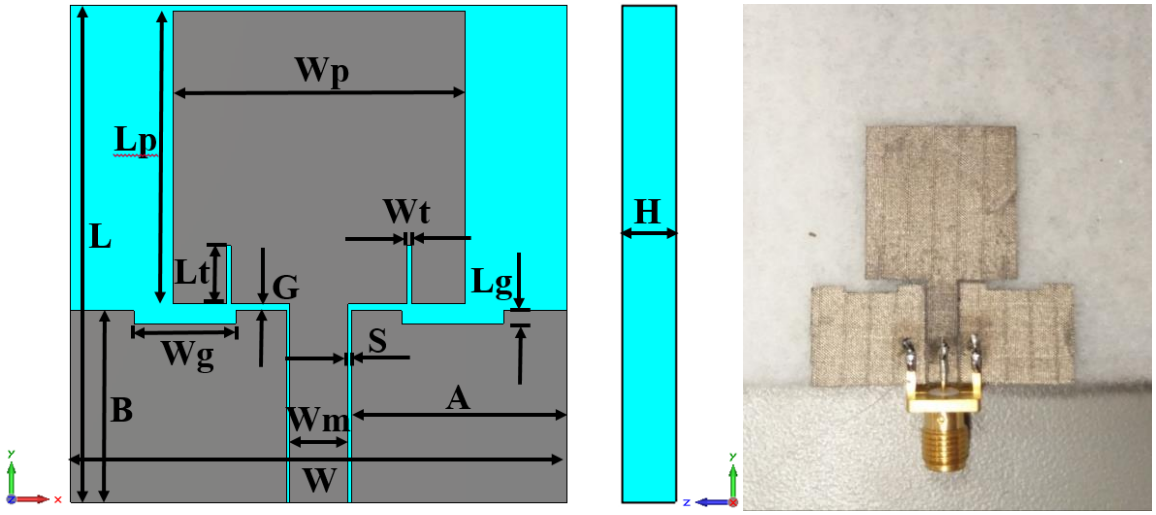

(a) (b)

Figure 20: CPW-fed monopole antenna, (a) geometry, and (b) fabricated prototype.

Table 3: Parameters of CPW-fed monopole antenna shown in Figure 20. Dimensions are given in mm.

Parameters	Dimension (mm)
L	34.00
W	34.00
L_P	20.00
W_P	20.00
L_T	4.00
W_T	0.35
L_G	0.90
W_G	6.96
A	14.8
B	13.6
D	4.00
S	0.20
W_M	4.00
G	0.46
H	1.80

Figure 21 depicts the measured and simulated reflection co-efficient of the antenna. Reflection coefficient measurements have been carried out using Agilent E5071C Network Analyzer. The simulation gives us an impedance bandwidth of 7.3 GHz starting from 2.7 GHz to 10 GHz, with -30 dB reflection co-efficient at 5.8 GHz. In the measurement result we can notice that the impedance bandwidth reduces. This is due to the error in fabrication and matching error while measurement. However from the measurement the impedance bandwidth is found to 4.5 GHz, starting from 4 GHz to 8.5 GHz. The reflection Co-efficient at 5.8 GHz is -10.8 dB.

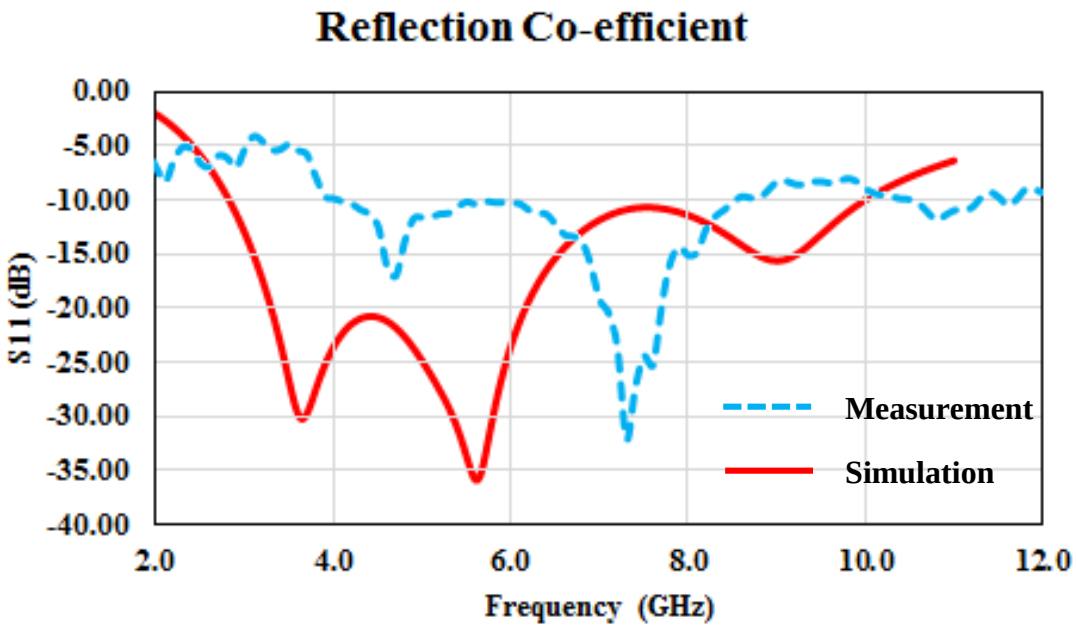

Figure 21: Simulated and measured reflection co-efficient of the CPW-fed antenna.

Furthermore, radiation patterns measurements have been performed using the anechoic chamber in Antenna Measurements Laboratory at University of North Dakota. Figure 22 shows the E-plane radiation pattern of the monopole antenna at 5.8 GHz based on simulation and measurement results. It's worth mentioning that the simulated cross-pole

component isn't shown in the figure since it has a low value that is less than -80 dB. Figure 23 shows the simulation and measurement results of the H-plane radiation pattern of the antenna alone at 5.8 GHz. The simulated antenna gain is 1.17 dBi while the measured value is 2.97 dBi, which means an improvement by 1.8 dBi. Also, an increament of 1 dB in the antenna gain is obtained from the measured radiation pattern in H-plane as compared with simulated value.

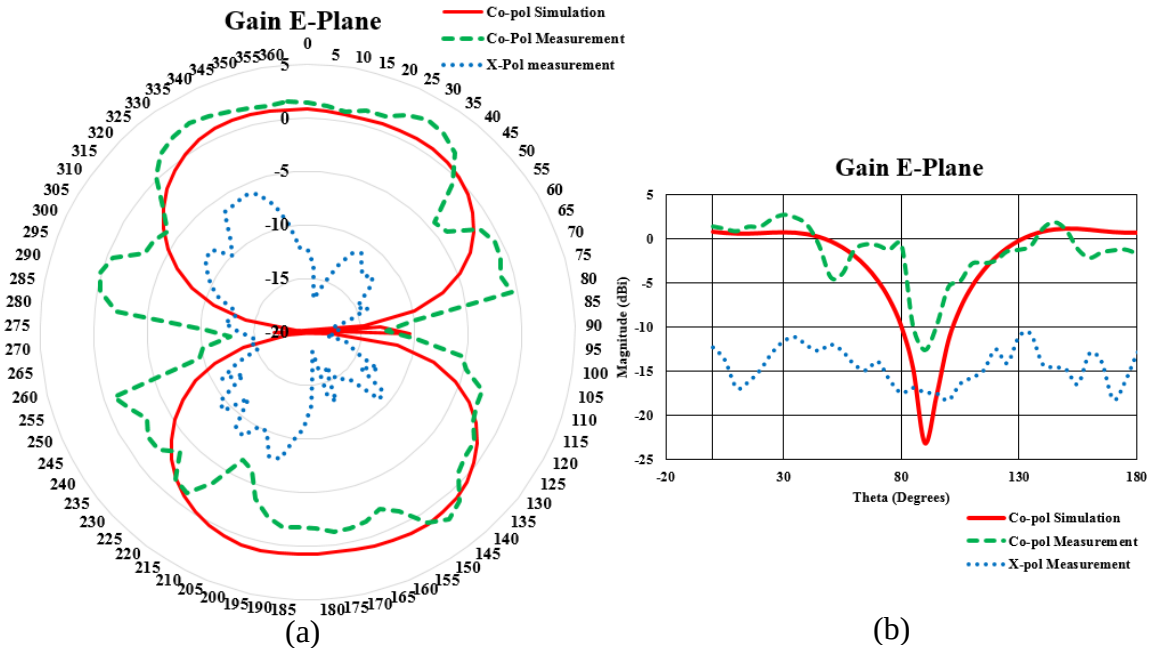

(a) (b)

Figure 22: E-plane gain of the antenna (a) Polar plot, and (b) 2D plot.

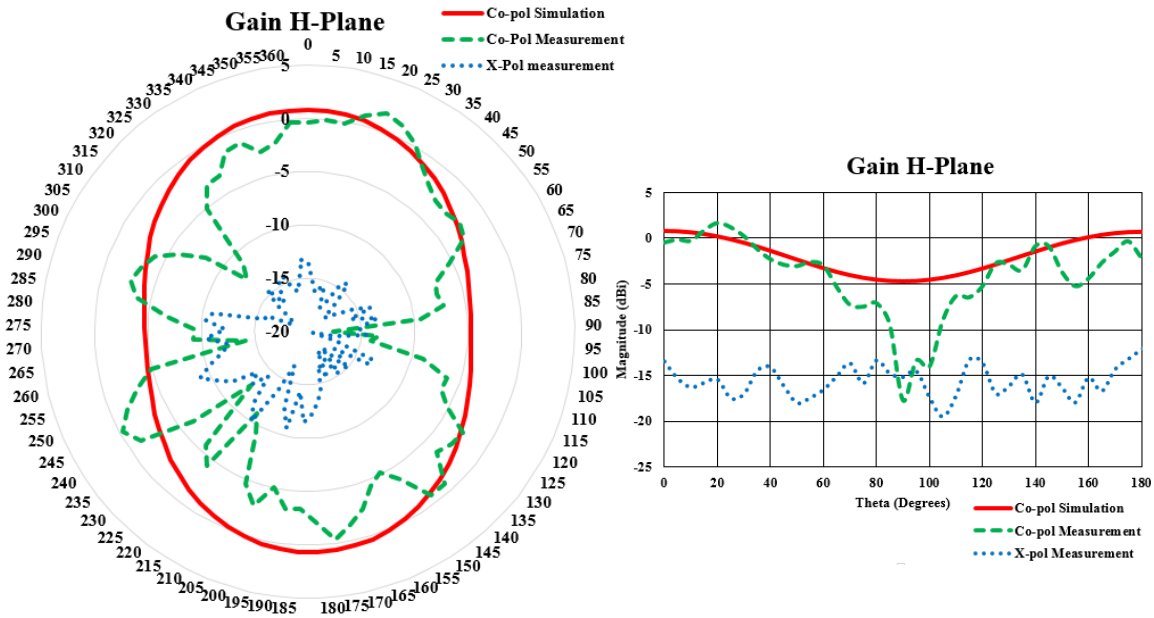

(a) (b)

Figure 23: H plane gain of the antenna alone (a) Polar plot, and, (b) 2D plot.

3.3 Geometry of the EBG Unit Cell and Reflection Phase Characteristic

In this part geometry and dimensions of the EBG unit cell will be discussed. Addition to that the simulation results of the phase reflection characteristic will also be discussed. The geometry of the EBG unit cell is based on the proposed design in [83]. The design is based on a fractal shape. The shape is known as the first order Peano curve. A flexible substrate, Rogers 3003 material, with a thickness of 1.52 mm, relative dielectric permittivity of 3 and electrical loss tangent of 0.001 is used for the design of the EBG. Figure 24 and Table 4 show the dimensions (in mm) of a single cell of the EBG structure. CST Microwave Studio is used for the simulation of the EBG.

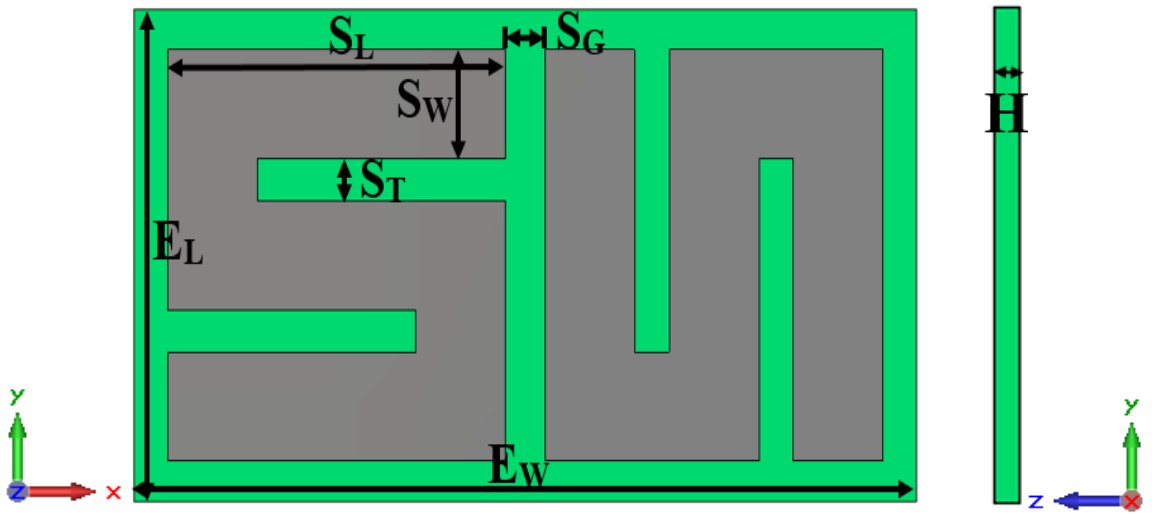

Figure 24: Geometry of the proposed EBG cell.

Table 4: Parameters of EBG unit cell shown in Figure 22. Dimensions are given in mm.

Parameters	Dimension (mm)
E_L	31.60
E_W	61.10
S_L	26.40
S_W	7.00
S_G	3.10
S_T	2.70
H	1.52

The EBG structure is designed by means of reflection phase characterization. The reflection phase is examined with the simulation model shown in Figure 25. In order to search for the AMC in phase band, a single cell with Periodic Boundary Conditions (PBC) in *x* and *y* directions was simulated.

Figure 26 shows the calculated reflection phase diagram of EBG structure. As the frequency increases the phase decreases continuously from 180° to -180°. At low and high frequency regions, EBG structure shows a similar phase to a perfect electric conductor

case, which is 180°. The EBG reflection phase is 0° at the resonance frequency, which resembles the unique property of EBG surface. The useful bandwidth of EBG surface has been defined by the range +90° to -90°. Within this range, image currents are almost in phase rather out of phase, thereby, the reflected wave makes constructive interference with the radiated wave. In the proposed cell, the exact AMC point is located at 5.782 GHz, having a narrow bandwidth of 2 KHz (5.781 GHz to 5.783 GHz) within +90 to -90 phase values.

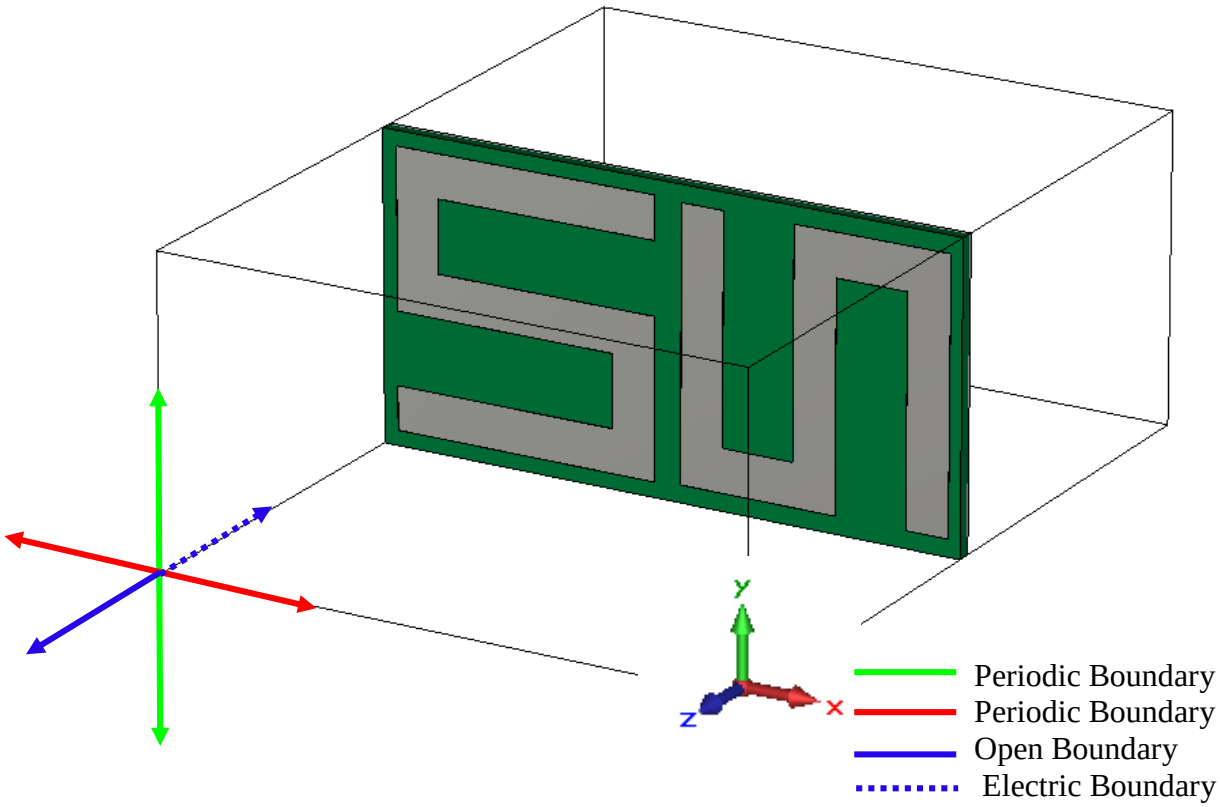

Figure 25: A unit cell simulation model set up for reflection phase analysis.

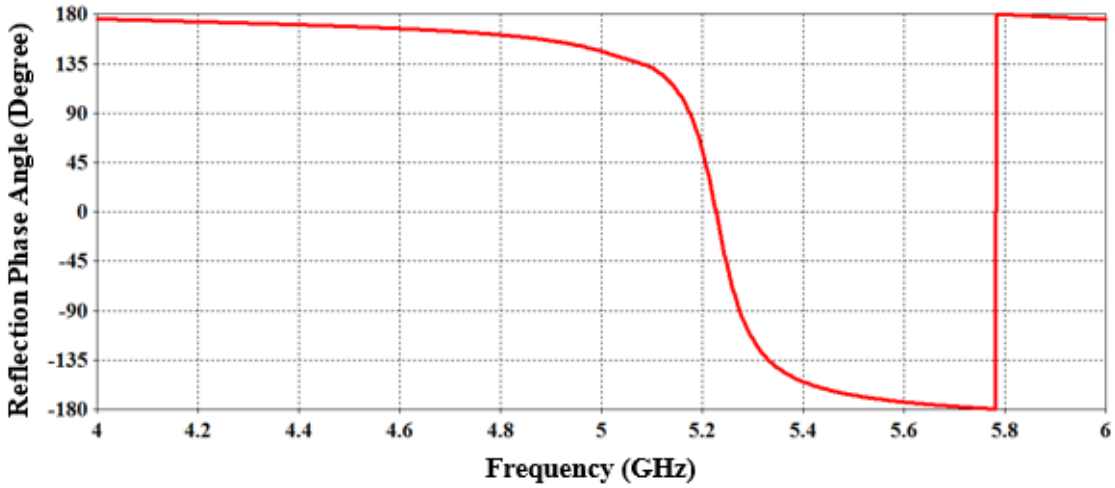

Figure 26: Reflection phase diagram of an EBG cell at normal incidence.

3.4 CPW Monopole Antenna Performance with EBG Structure

In this section the design, simulation and measurement results of the CPW monopole antenna integrated with the EBG structure will be discussed. For this design a 3 × 2 array of the EBG unit cell is used. The dimension of the EBG array is 122 mm × 94.8 mm. Figure 27 illustrates the design of the EBG array structure. The array size was increased by one row and one column at a time until satisfactory performance was achieved in terms of high gain within the frequency range of interest and relatively small size. Figure 28 shows the integration of the antenna with EBG.

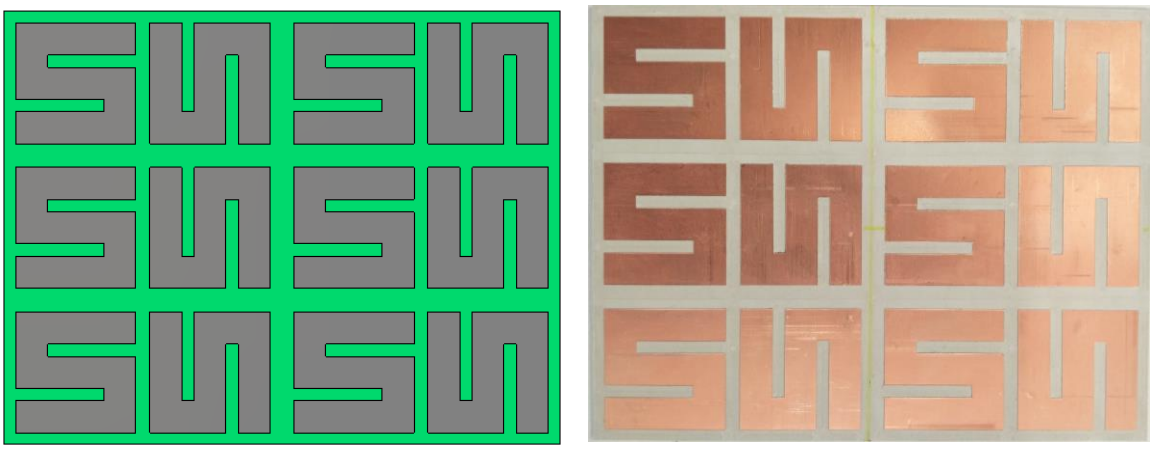

(a) (b)

Figure 27: 3 × 2 array of the EBG unit cells: (a) simulated, and (b) prototype.

The EBG array structure is cut out of a 12 inch × 9 inch of RO3003 sheet. Milling machine is used for cutting purposes. The copper clading on the sheet is 7.5 µm.

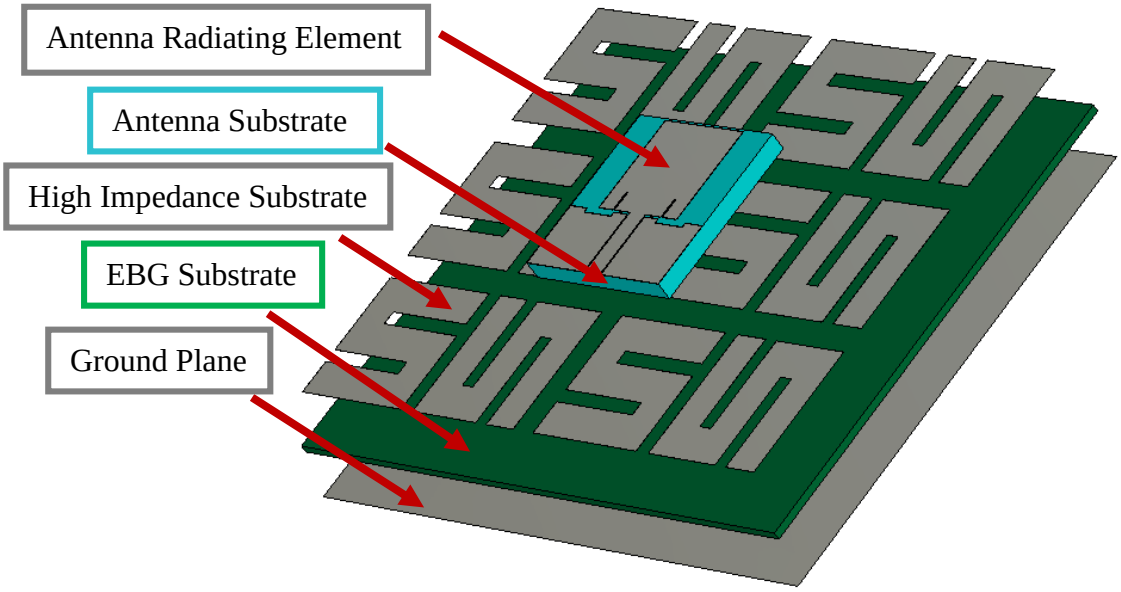

Figure 28: CPW monopole antenna on EBG structure.

By comparing the antenna gain with and without EBG structure the effectiveness and usefulness of the EBG ground plane can be assessed. A few important observations can be made from the results shown in Figures 29 and 30. In Figure 29 (a) and (b) illustrate

the 3D realized gain at 5.8 GHz for conventional monopole antenna and the antenna integrated on AMC.

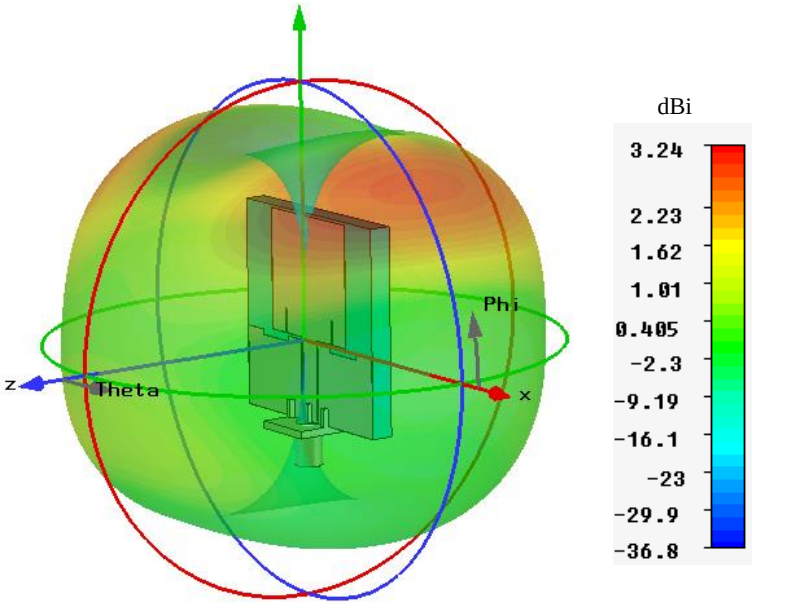

(a)

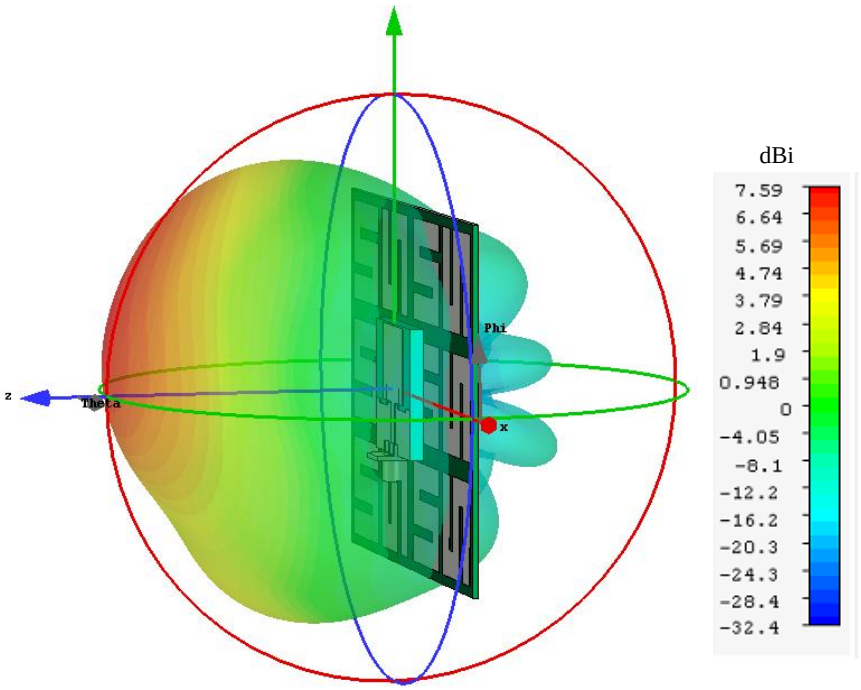

(b)

Figure 29: 3D patterns at 5.8 GHz of (a) monopole antenna, and (b) antenna integrated with the EBG.

Figure 30 (a) and (b) show the E-plane and H-plane radiation patterns at 5.8 GHz, for conventional monopole antenna and the antenna integrated on EBG, respectively. As it was expected, the backward radiation of the antenna is reduced significantly by EBG, hence the gain is considerably improved. The antenna on EBG has a realized gain of 7.28 dBi, while the antenna alone shows 1.17 dBi gain. This means improvement of 522% in antenna gain using the EBG. Furthermore, FBR is a critical factor in wearable antennas. FBR increased from 0.09 dB in the conventional monopole antenna to 21.87 dB using the EBG structure.The radiation patterns at 5.8 GHz show the improvement in the antenna gain and directivity as well. Antenna directivity has been increased from 1.25 dB to 7.8 dB using EBG structure. However, the power level of the cross-pol components of the antenna's field has been increased using EBG, which is usually undesirable.

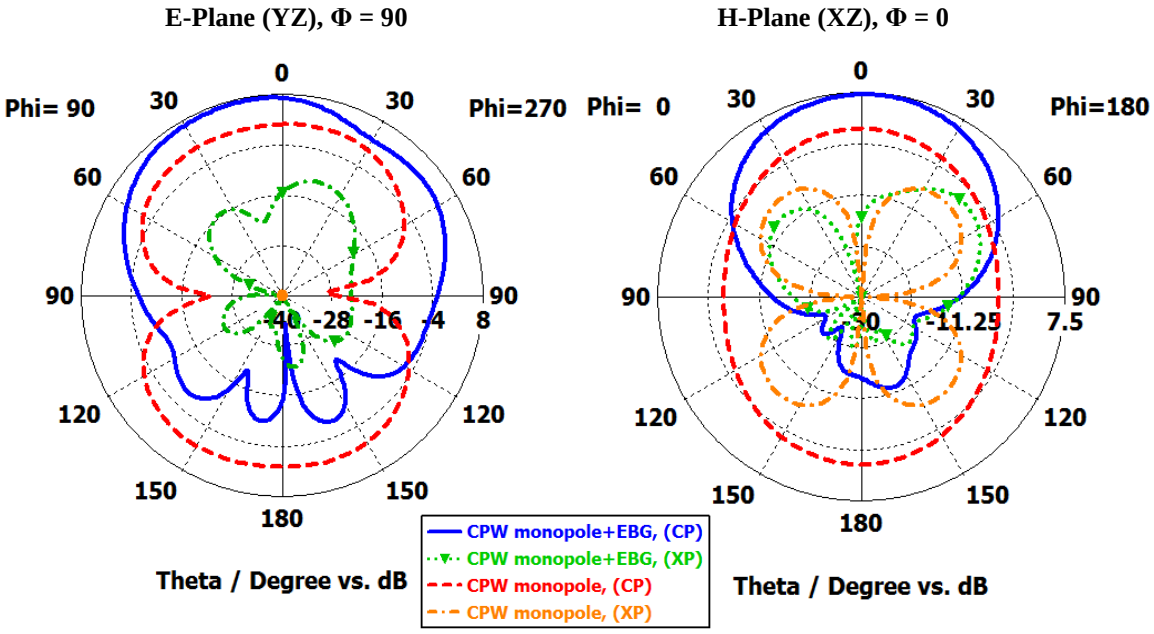

Figure 30: Simulated radiation patterns of monopole antenna with and without EBG structure at 5.8 GHz: (left) E-plane and (right) H-plane; Co Polarization (CP) and Cross Polarization (XP).

Simulated reflection coefficient of the proposed antenna with EBG is compared with the measured one as shown in Figure 31. It can be observed that there is an improvement in the reflection co-efficient based on the measurement results. In simulation the value is -10.59 dB and in measurement it shows -14.53 dB at 5.8 GHz. The impedance bandwidth for measurement is 4.3 GHz (4.2 GHz to 8.5 GHz), whereas the simulation result shows an impedance bandwidth of 4.6 GHz (5.3 GHz to 9.9 GHz).

On the other hand, a significant reduction in the impedance bandwidth of monopole antenna by about 2.4 GHz (based on simulation) due to the usage of EBG structure, which makes it hard to compare both results in the same figure. However, the obtained bandwidth of EBG antenna is obviously covering the ISM-5.8 GHz band with a good matching characteristics.

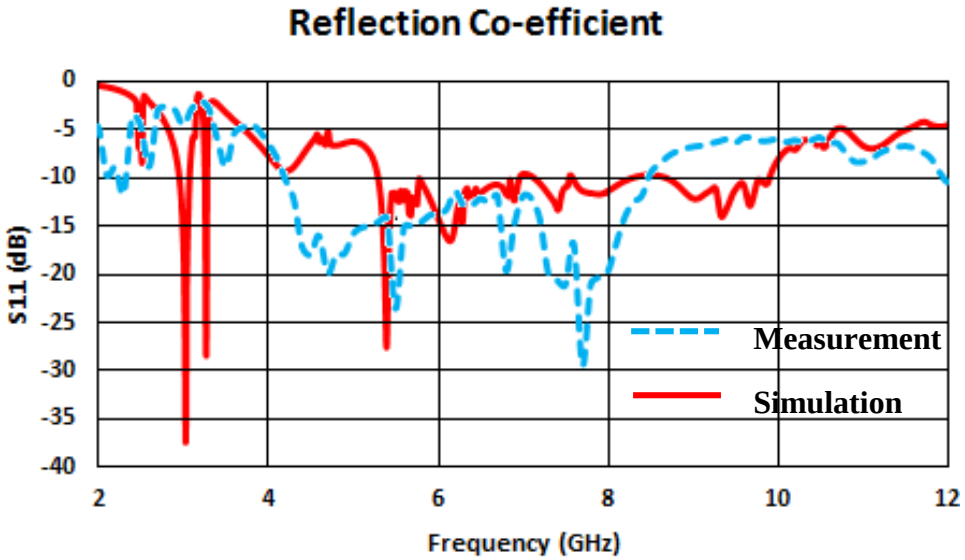

Figure 31: S_{11} results of the antenna with EBG structure integrated.

Figures 32 and 33 show the comparison between simulation and measured radiation pattern of the antenna with EBG structure.

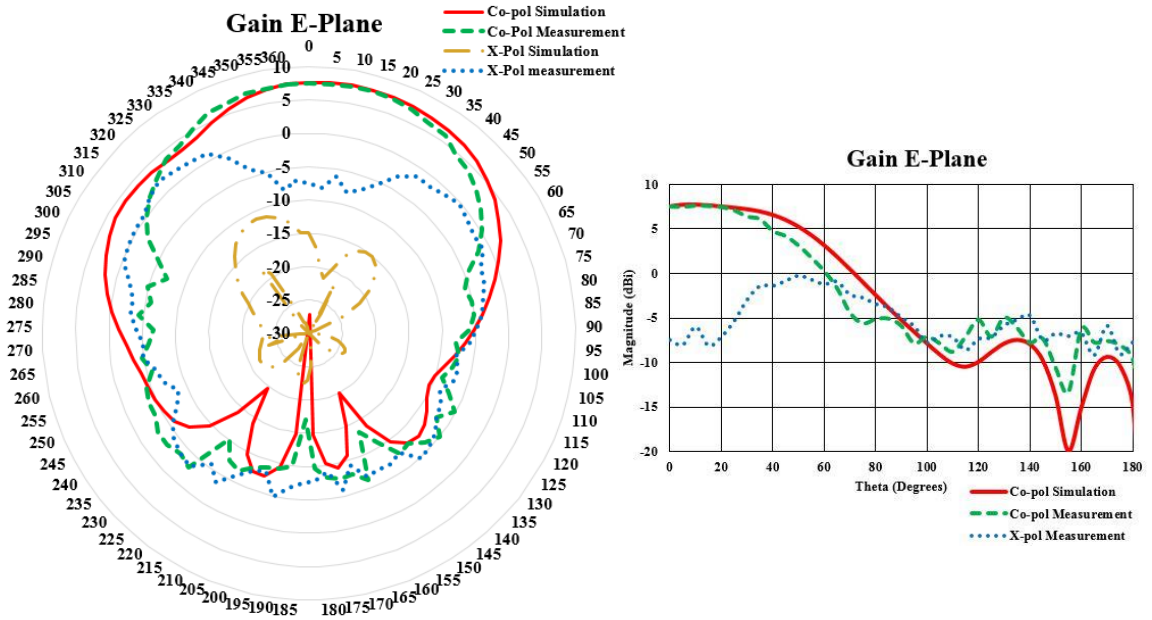

(a) (b)

Figure 32: E plane Gain of the antenna with EBG (a) polar plot and, (b) 2D plot.

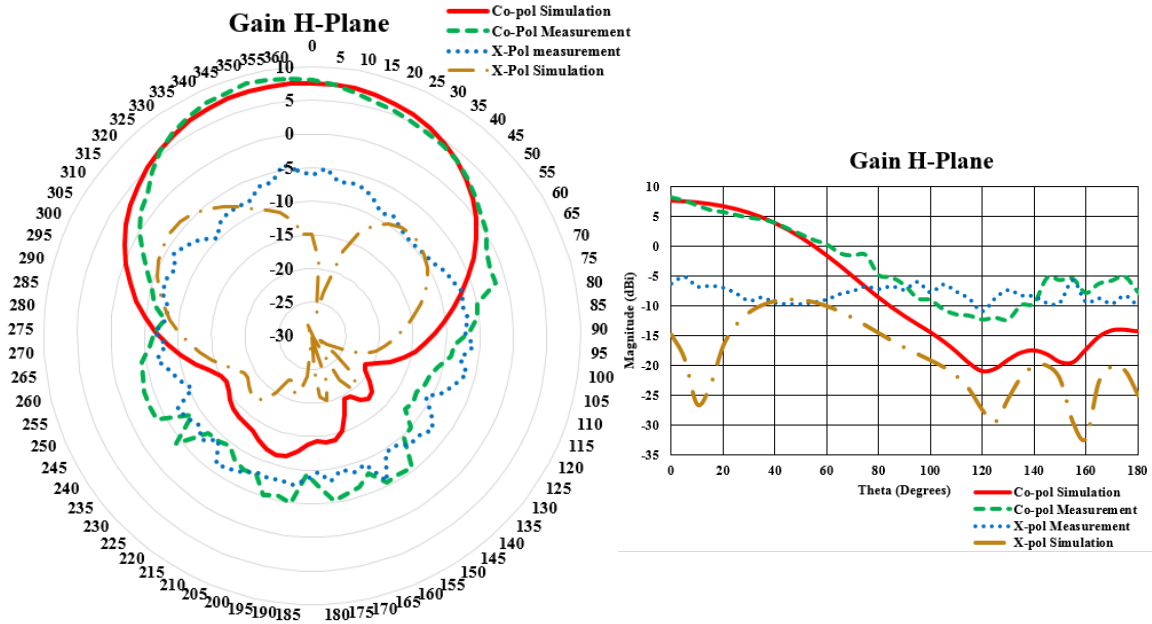

(a) (b)

Figure 33: H-plane gain of the antenna with EBG, (a) polar plot and, (b) 2D plot.

These figures show the co-polarization and cross-polarization of E-plane and H-plane radiation patterns of the antenna on EBG. From Figures 32 and 33 it can be seen

that the E-plane gain for measurement result at 5.8 GHz is 7.76 dBi which is very close to the simulation value of 7.28 dBi. Also the FBR of the measured antenna with EBG structure is 13.2 dB, which is 10.28 dB higher than the measured antenna alone. This means the antenna with EBG is more directive. The cross-polarization of the 2D plot of the E-plane is not shown because of it is very small value.

Table 5 presents a comparison of the results on the single antenna without EBG and antenna with EBG structure. The comparison is based on the simulation and measurement results.

Table 5: Comparison of performances on antenna on free space and antenna on EBG simulation and measurement.

Parameter	Antenna alone simulation	Antenna alone measurement	EBG+antenna simulation	EBG+antenna measurement
Size $(L \times W)$ **mm**^{2}	34×34		122.2×94.8	
f_l (GHz)	2.8	3.9	5.3	4.2
f_h (GHz)	10.1	8.8	9.9	8.5
f_r (GHz)	5.6	7.3	5.4	7.7
Gain @ 5.8 GHz (dBi)	1.17	2.97	7.28	7.76
S_{11} @ f_r (dB)	-35.00	-32.12	-27.52	-29.41
S_{11} @ 5.8 GHz (dB)	-30.76	-10.17	-10.59	-14.53
FBR (dB)	0.09	2.92	21.87	13.2

3.5 CPW Monopole and EBG Integrated Antenna Performance on Spacesuit Structure

The antenna and EBG performance are also examined on the spacesuit material. As the ultimate goal is to integrate the antenna with EBG on the spacesuit of the astronauts. For this purpose University of North Dakota's NDX-II spacesuit [84] was considered. To reduce the effects of bending and crumbling condition the chest part of the suit is considered to be optimum place to integrate the antenna with the EBG. From the measurement of the spacesuit it was found that the dimension of this part is 13 × 2 cm^2. The outer layer of the spacesuit is made out of Ortho-fabric. The effects of the stainless steel rings in the spacesuit are also taken into account. Figures 34 and 35 show the simulated structure of the spacesuit and the integration of antenna and EBG on the spacesuit material, including the fabric and aluminum.

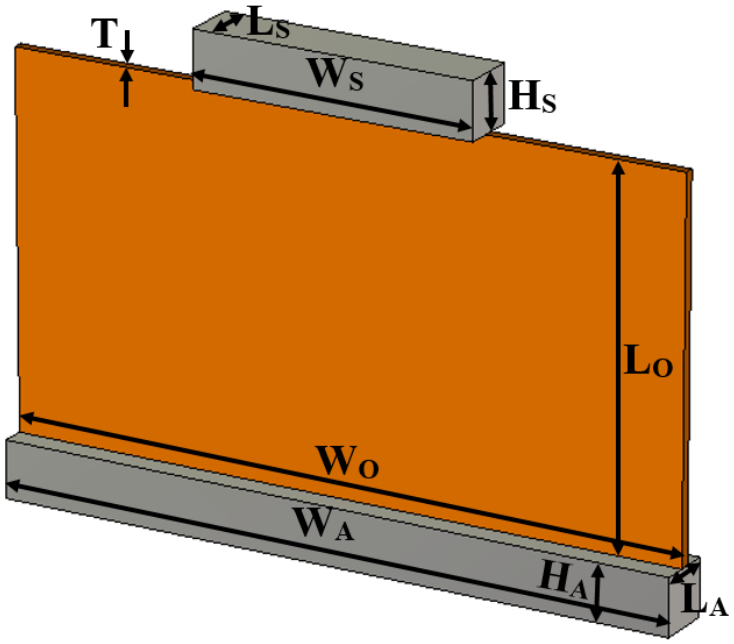

Figure 34: Simulation model of the chest part of the spacesuit.

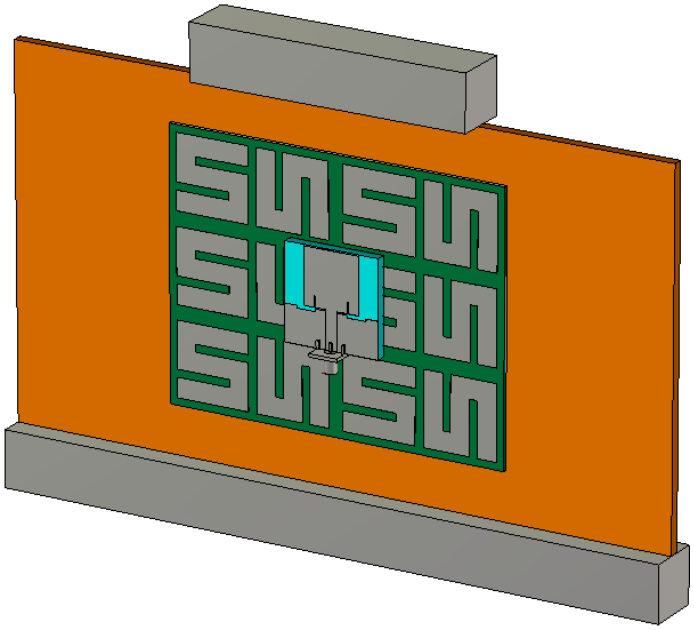

Figure 35: Integration of the antenna and EBG on the spacesuit material.

In Table 6 the parameters of the spacesuit structure are listed.

Table 6: Parameters of the space suit structure

Parameters	Dimension (mm)
W_A	240
L_A	20
H_A	20
W_O	240
L_O	130
T	3.6
W_S	100
L_S	20
H_S	20

Figure 36 shows the comparison result of S_{11} parameters of the antenna alone in free space and antenna on spacesuit material.

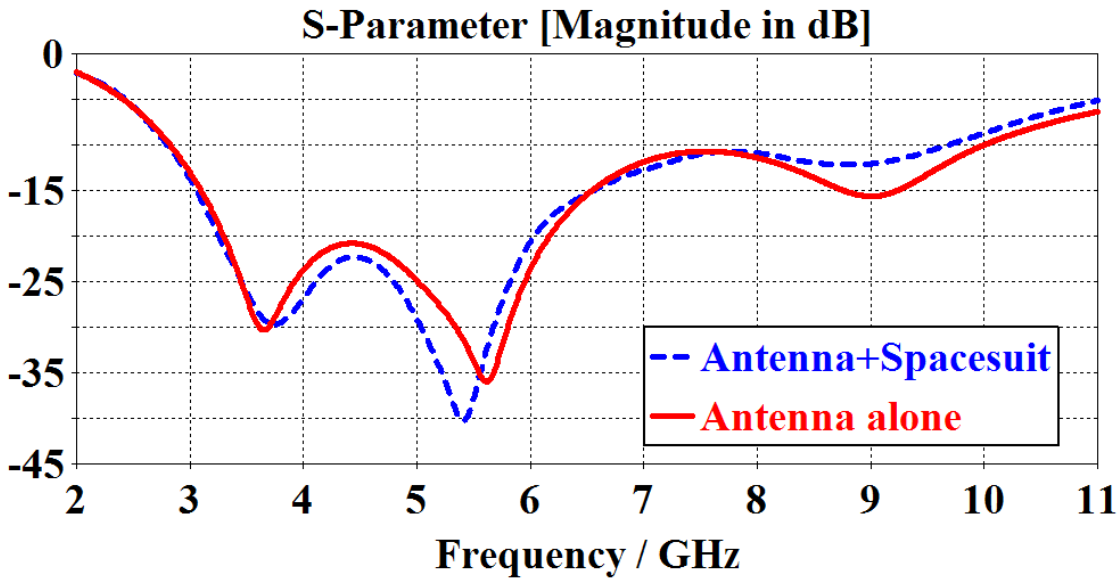

Figure 36: Reflection co-efficient of the antenna in free space and on spacesuit.

It can be noticed that the impedance bandwidth of the antenna on spacesuit is reduced by 0.3 dB (From 2.7 dB to 9.7 dB) compared to the antenna in free space. The reflection co-efficient at 5.8 GHz is reduced to -25.6 dB for antenna on spacesuit compared to -30 dB of the antenna in free space.

From the Figure 37 (a) and (b) and Figure 38 (a) and (b) the information about the co-polarization and cross-polarization of the E-plane and H-plane can be obtained. It can be noticed from Figure 37 that the realized gain of the E–plane of the antenna on spacesuit has about 0.5 dB increment in co-polarization level (from 1.16 dBi to 1.63 dBi) and almost 3 dB (-98.4 dBi to -95.1 dBi) increment in the cross-polarization compared to the antenna in free space. On the other hand, similar performance is also found in Figure 38, which shows about 0.5 dB increment in co-polarization and 3 dB increment in cross-polarization of the H-plane.

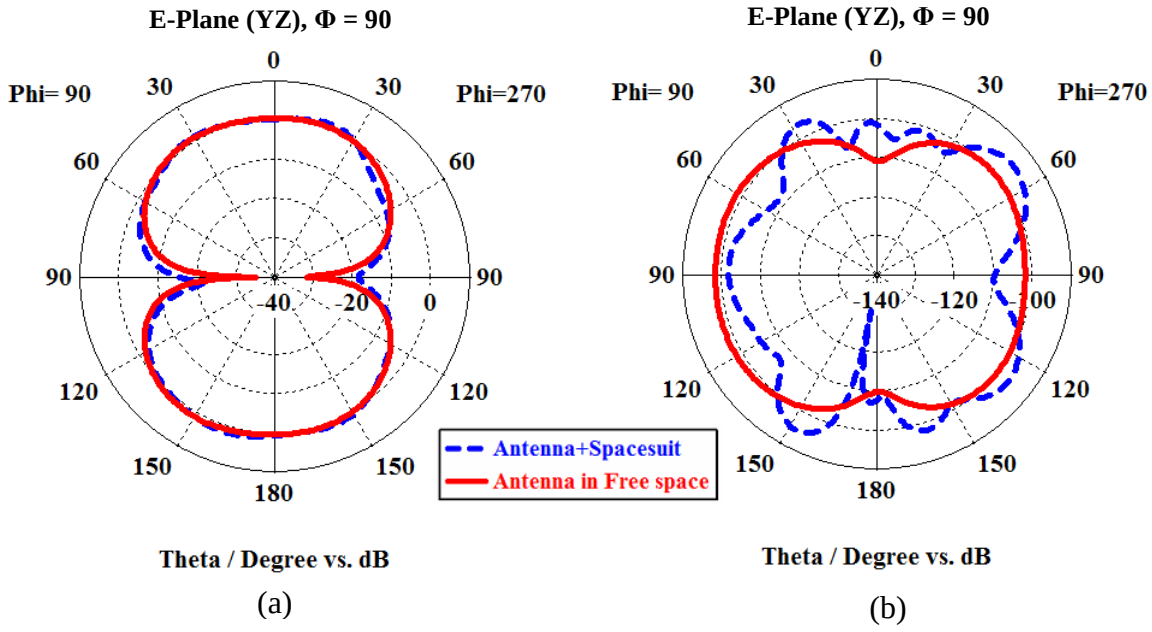

(a) (b)

Figure 37: Simulated E-plane radiation patterns of monopole antenna with and without spacesuit material at 5.8 GHz (a) co-polarization, and (b) cross polarization.

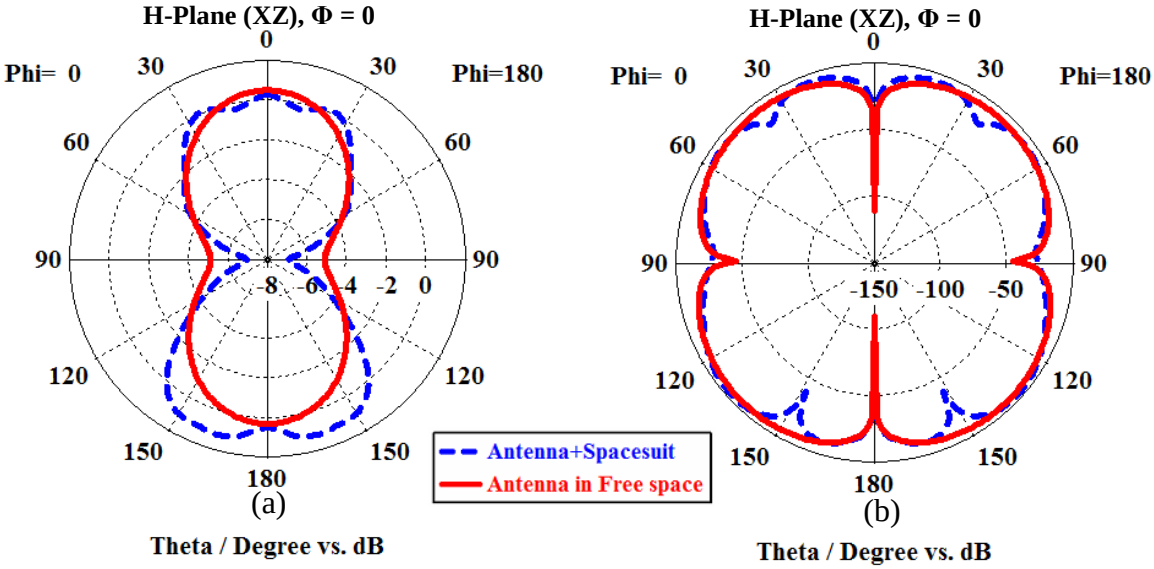

(a) (b)

Figure 38: Simulated H-plane radiation patterns of monopole antenna with and without spacesuit material at 5.8 GHz: (a) co-polarization, and (b) cross-polarization.

Next, the performance of the antenna with EBG structure on spacesuit is discussed. From Figure 39 it can be seen that by using the EBG structure the effects of the spacesuit material on the antenna becomes almost negligible. The S-parameter results shows very similar performance of the EBG antenna with and without the spacesuit material. The reflection coefficient at 5.8 GHz is -10.59 dB and -12.85 dB, respectively for EBG antenna and EBG antenna on spacesuit. The impedance bandwidth at -8 dB of the EBG antenna on spacesuit is about 4.6 GHz, which is same as the EBG antenna in free space at -10 dB.

Figure 40, 41 and 42 illustrates the radiation pattern of the E-plane and H-plane of the EBG antenna in free-space and EBG antenna on spacesuit. The realized gain is 7.28 dBi and 6.38 dBi for the EBG antenna in free space and EBG antenna on spacesuit, respectively.

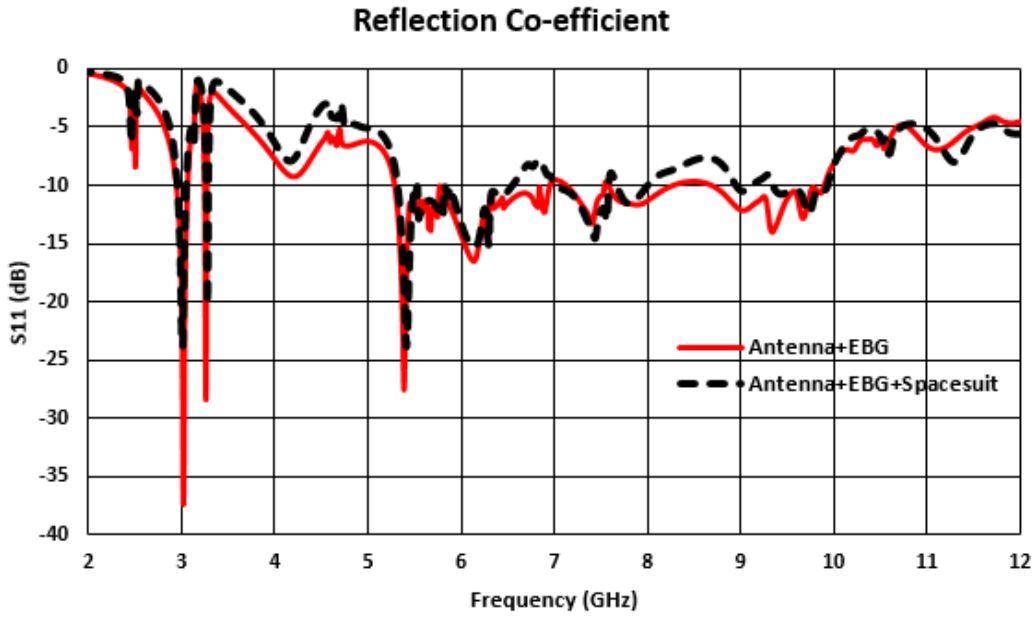

Figure 39: Reflection co-efficient (S_{11}) of the antenna integrated with EBG in free-space and on the spacesuit material.

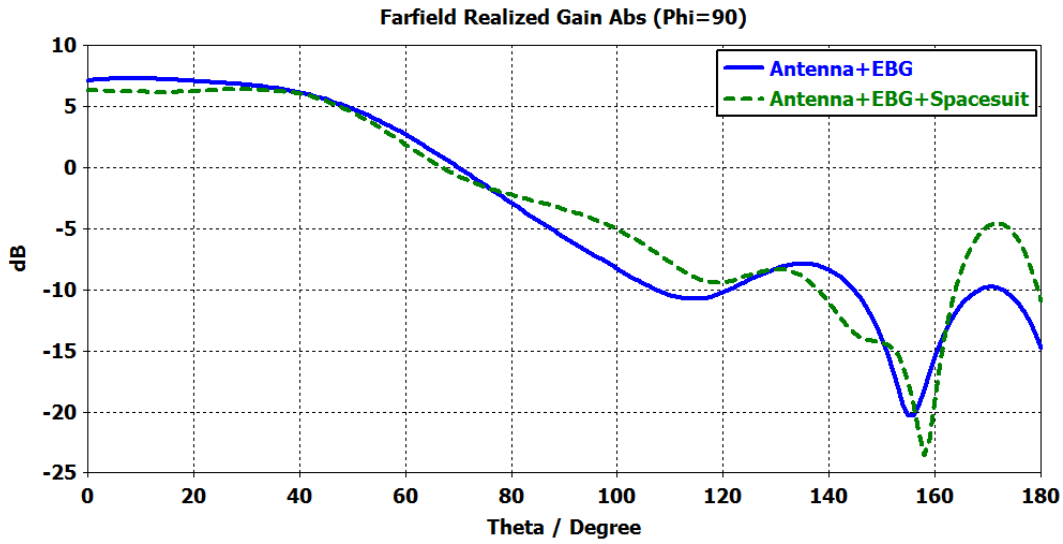

Figure 40: E-plane realized gain.

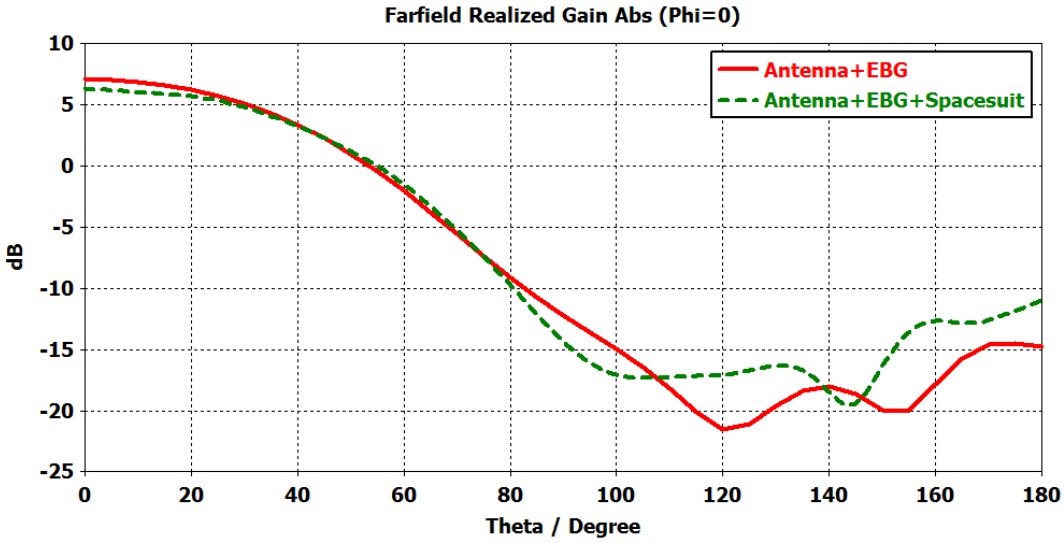

Figure 41: H-plane realized gain.

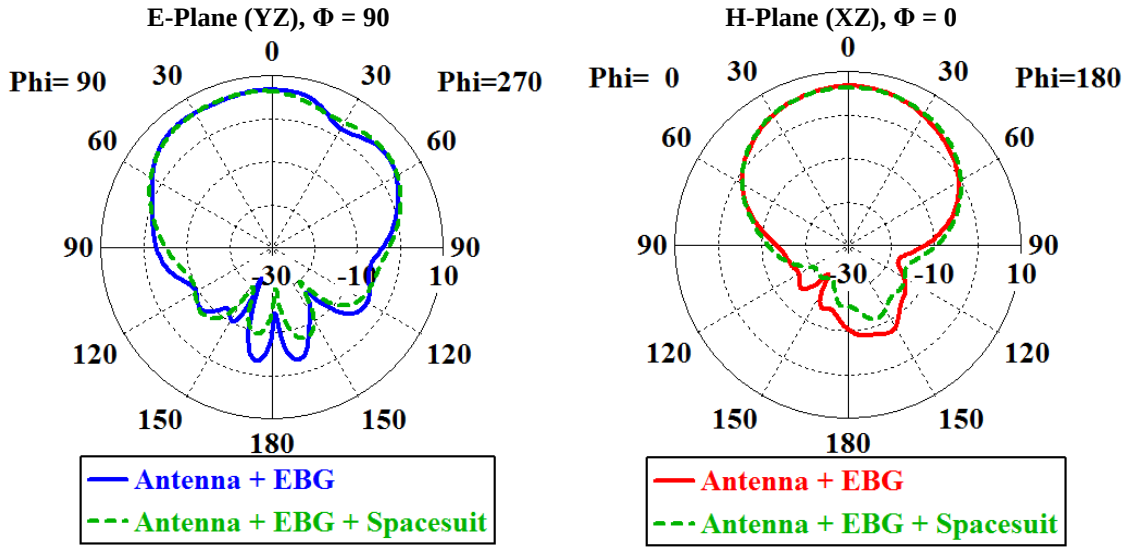

(a) (b)

Figure 42: Comparison of gain patterns of the antenna integrated with EBG in free-space and on the spacesuit, (a) E-plane, and (b) H-plane.

The comparison of co-polarization and cross polarization of the E-plane and H-plane of the EBG antenna with and without spacesuit is illustrated in Figure 43. The FBR of the EBG antenna on spacesuit is 17.75 dB, which is around 5 dB less than the EBG antenna in free space (22.23 dB). This FBR is still better than that for a single antenna in free space, which ensures that there is minimum back radiation. This is important to make sure the astronauts are less exposed to the electromagnetic waves of the antenna.

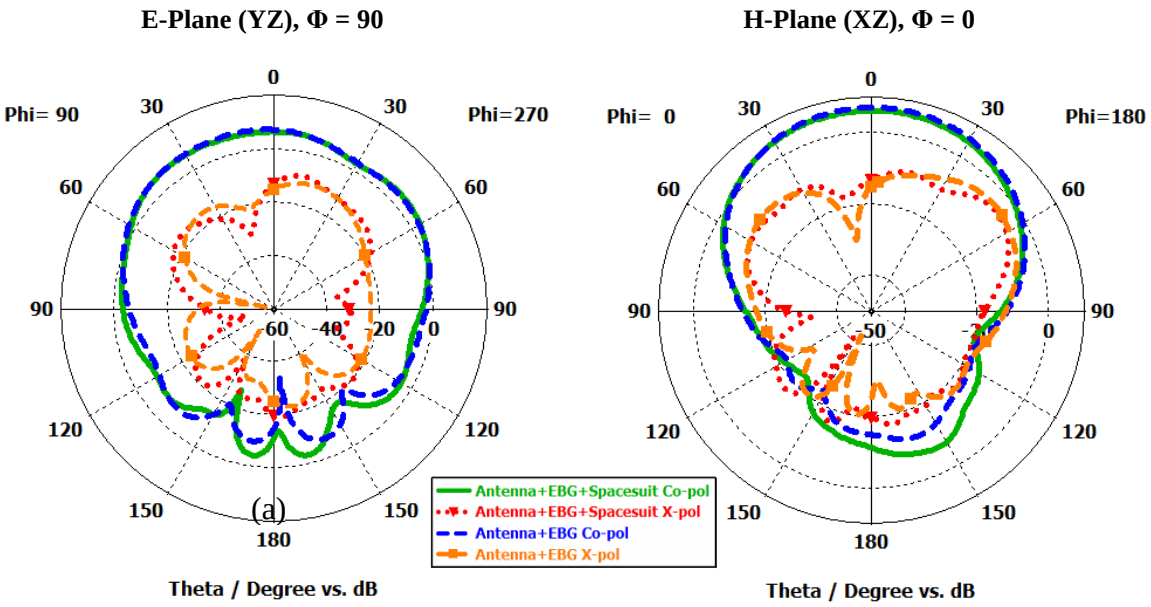

(a) (a) (b)

Figure 43: Antenna radiation patterns (a) E-plane and, (b) H-plane.

CHAPTER IV

ANTENNA PERFORMANCE UNDER STRETCHING CONDITION

4.1 Introduction:

In the harsh environment of outer space like vacuum and extreme temperature to keep a human alive a space suit is worn as a garment. As a safety precaution flight jackets are worn inside the spacecraft. For extravehicular activity (EVA), which means work done outside spacecraft, it is mandatory to wear spacesuit. With a complex system of equipment and environmental systems the modern spacesuits have developed the basic pressure garment. It is designed keeping in mind the comfort level of the wearer. Additionally minimizing the effort required to bend the limbs is also an important parameter for the design. Independent of the spacecraft, a self-regulating oxygen supply and environmental control system is installed to allow complete freedom of movement.

Commonly, to confirm enough oxygen is supplied for respiration, a pressure of about 32.4 kPa (4.7 psi) is required for a space suit that is using pure oxygen. It is actually an addition of the partial pressure of oxygen in the earth's atmosphere at sea level 20.7 kPa (3.0 psi), 5.3 kPa (0.77 psi) CO_2 and 6.3 kPa (0.91 psi) water vapor pressure. In the spacesuits that use 20.7 kPa, there are 20.7 kPa − 11.7 kPa = 9.0 kPa (1.3 psi) of oxygen

that is available for the astronauts. This is almost the oxygen partial pressure attained at a height of 1,860 m (6,100 ft) above sea level, which is about the same pressure as in a commercial passenger jet aircraft. As a result, this is practically the lower limit of pressure for safe ordinary space suit pressurization.

The performance of the textile or flexible antennas can be affected by many factors such as bending, crumbling, stretching, temperature change, and humidity. Due to the pressure inside the spacesuit the fabric material tends to stretch. As the antenna is made up of textile, it will be prone to stretch due to the pressure. The estimated stretch is assumed to be up to 3% of its original size. The stretching was simulated for 3 cases: width only, length only, and width and length together.

In this chapter we will discuss the stretching effects on the performance of the antennas for 1%, 2% and 3% of width and length. Simulation results are presented for a single antenna element and antenna mounted the EBG layer. CST Microwave Studio has been used for the simulations.

4.2 Performance of the Stretched CPW Monopole Antenna

CPW monopole antenna's performance in free-space is investigated in details in Section 2 of Chapter 3. The results obtained in that section are for the antenna with its original dimensions. In this section antenna under different stretching conditions will be investigated for their performance to observe the changes in the radiation performance and the limitations for any stretching plane. Return loss and impedance bandwidth results for both E-plane (width) and H-plane (length) stretching will be presented. Moreover, radiation characteristics and radiation patterns at 5.8 GHz in the E and H planes of the antenna will

be presented as well. Geometry of the monopole antenna under stretching conditions in H-plane and E-plane individually and together are shown in Figure 44.

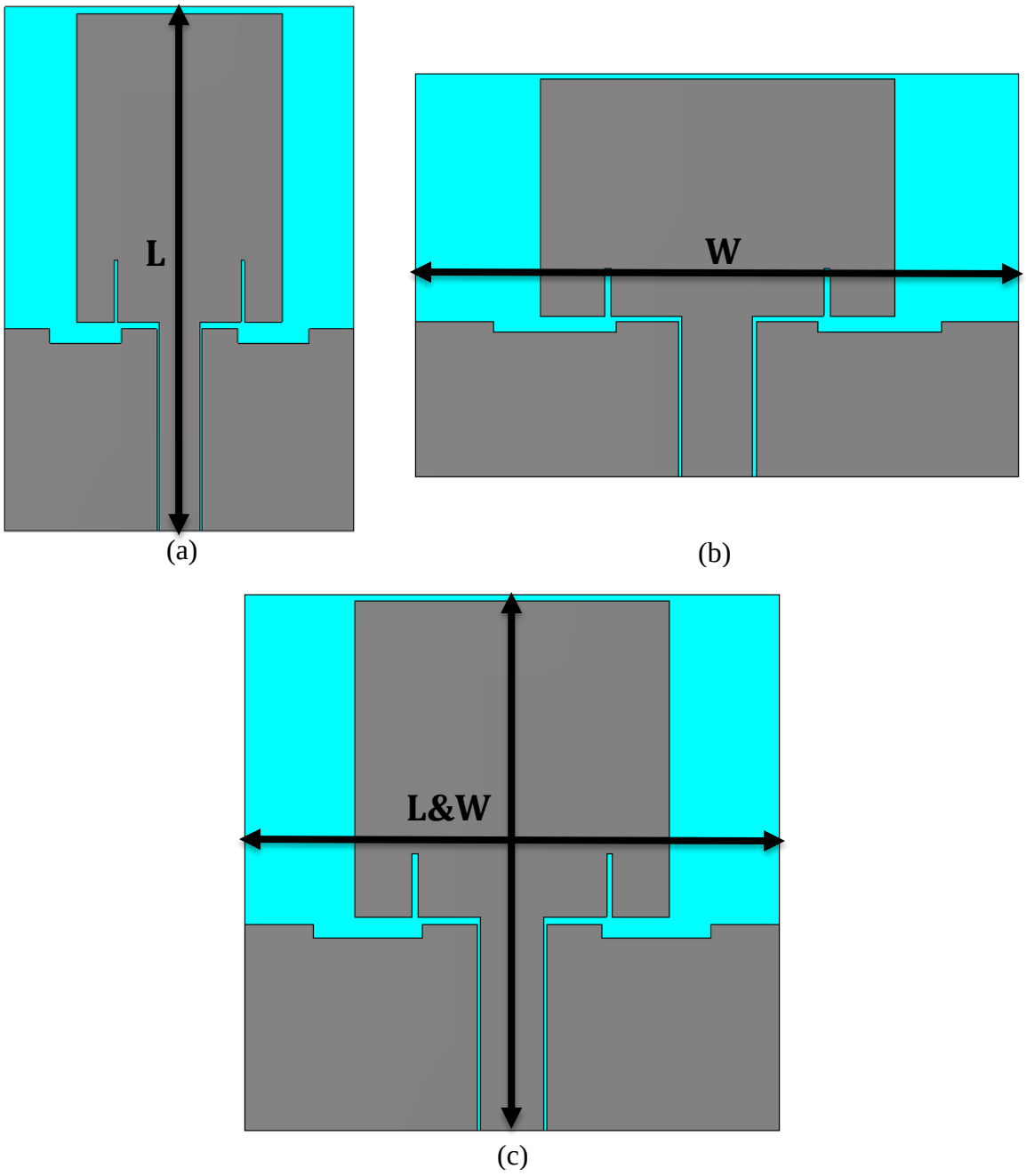

Figure 44: CPW monopole antenna stretched in (a) H-plane, (b) E-plane, and, (c) both E- and H-planes.

Figures 45-47 show the S-parameter of the CPW monopole antenna in free-space under different stretching conditions. It can be noticed that stretching in length or H-plane for up to 3% of the original length does not cause significant changes in the antenna performance. The performance almost similar to the original antenna is observed in Figure 45. However, when the antenna is stretched in width or E-plane the performance drops drastically, to the point that it was meaningless to compare the results with the original. Similarly stretching in both length and width together causes a lot of deteriorating effects in the antenna performance. Figure 48 shows the S-parameters for all cases in one plot.

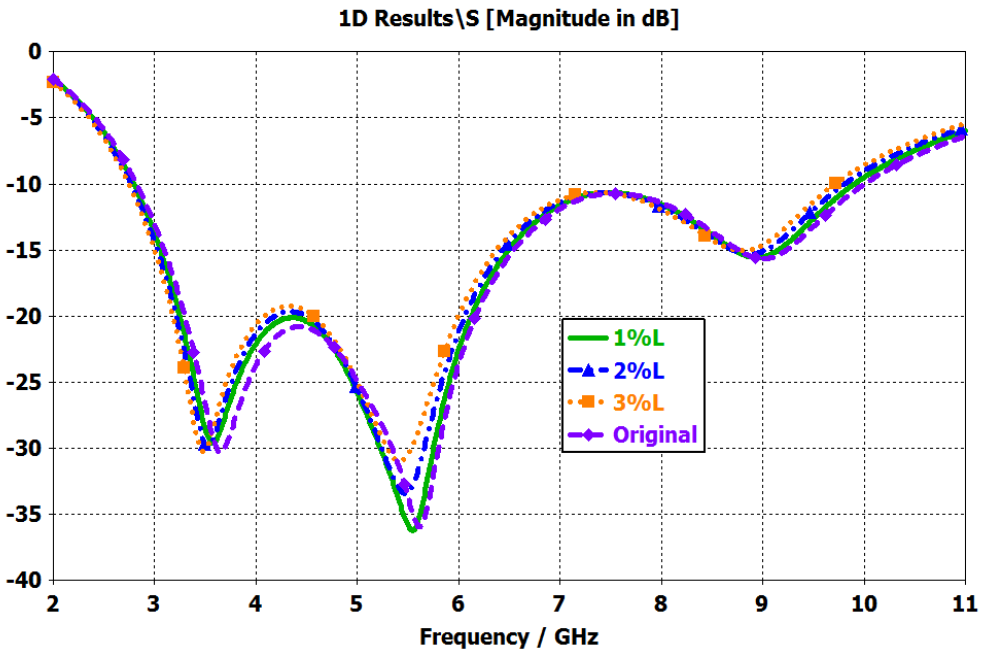

Figure 45: S parameter of the CPW antenna stretched in H-plane (L).

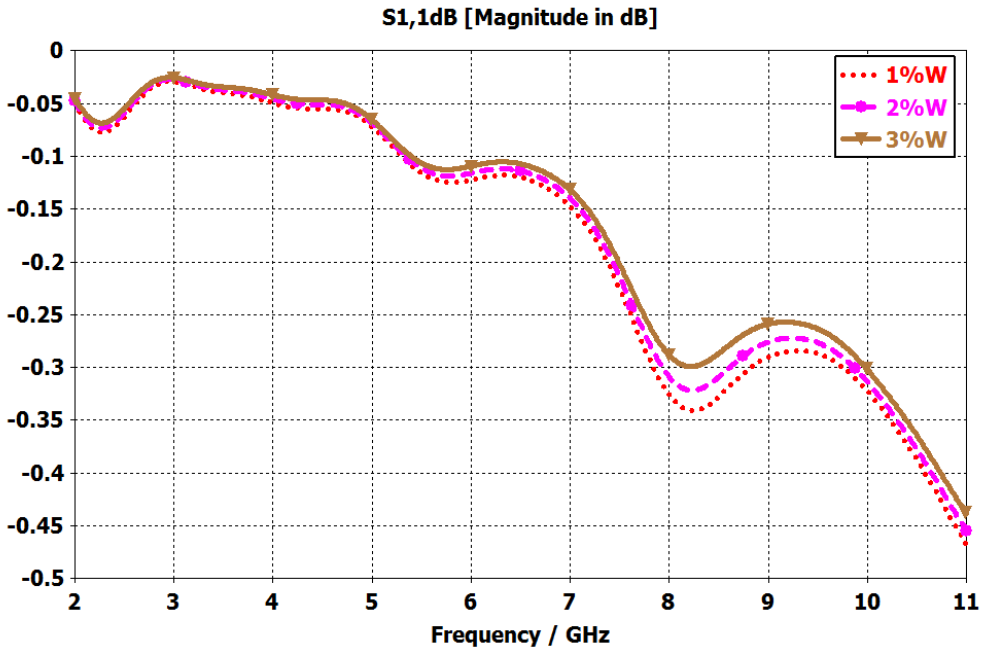

Figure 46: S parameter of the CPW antenna stretched in E-plane (W).

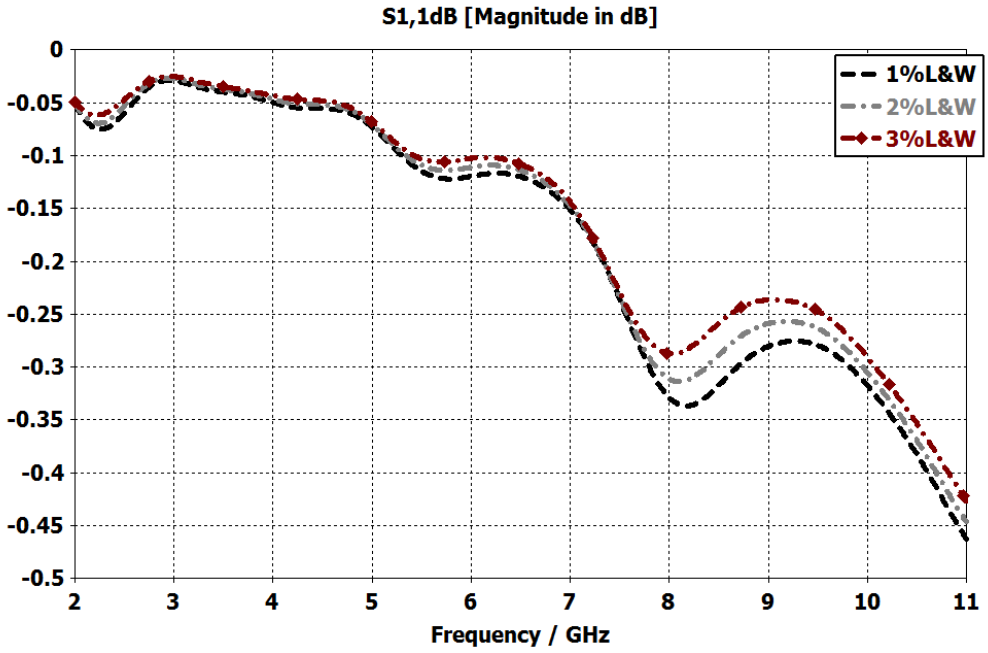

Figure 47: S parameter of the CPW antenna stretched in both E-plane and H-plane (L&W).

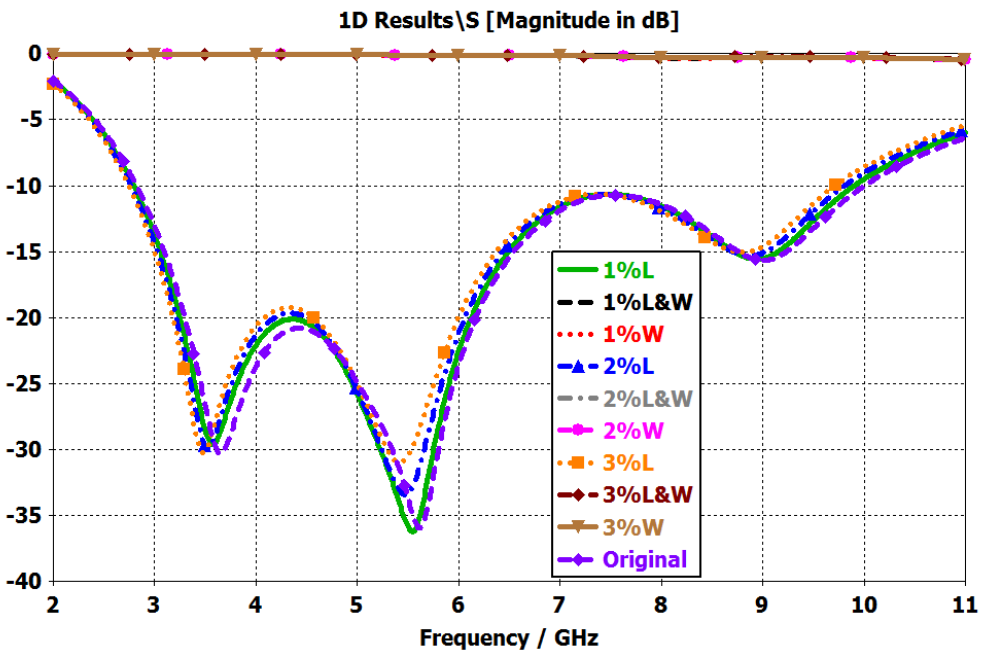

Figure 48: S-parameter comparision for stretching in different cases.

Figures 49-51 show the realized gain of the antenna in E-plane and H-plane when stretched in length, width and both length and width, respectively. Compared to the original antenna's radiation patterns it can be noticed that the gain remains almost the same when the stretching is done in length. However, the gain value decreases quite a bit when the antenna is stretched in width. When the stretching is done in both length and width together the realized gain value also drops drastically. All these results are summarized in Table 7.

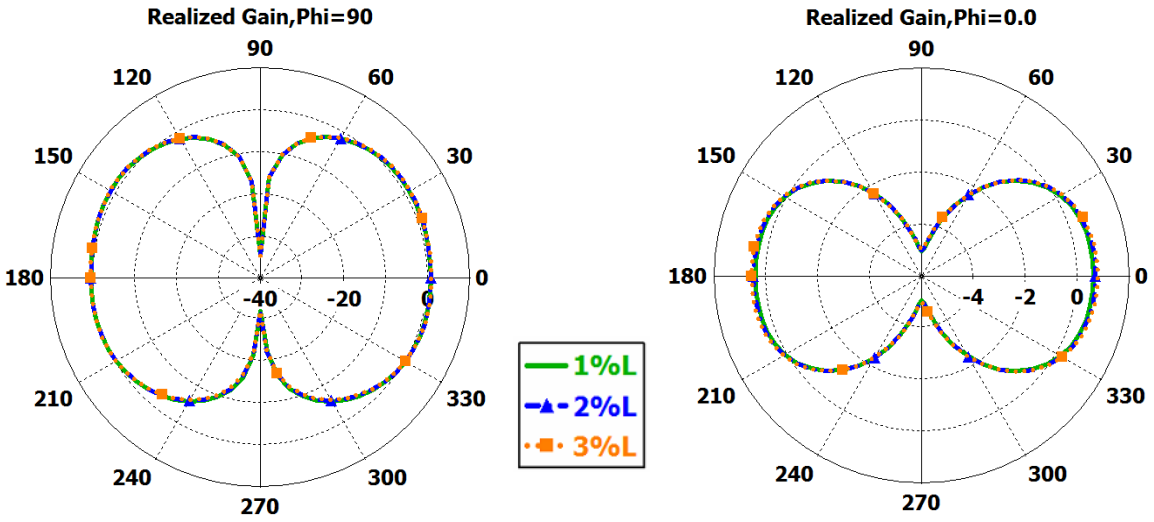

(a) (b)

Figure 49: Realized gain of the antenna stretching in length, (a) E-plane, and, (b) H-plane.

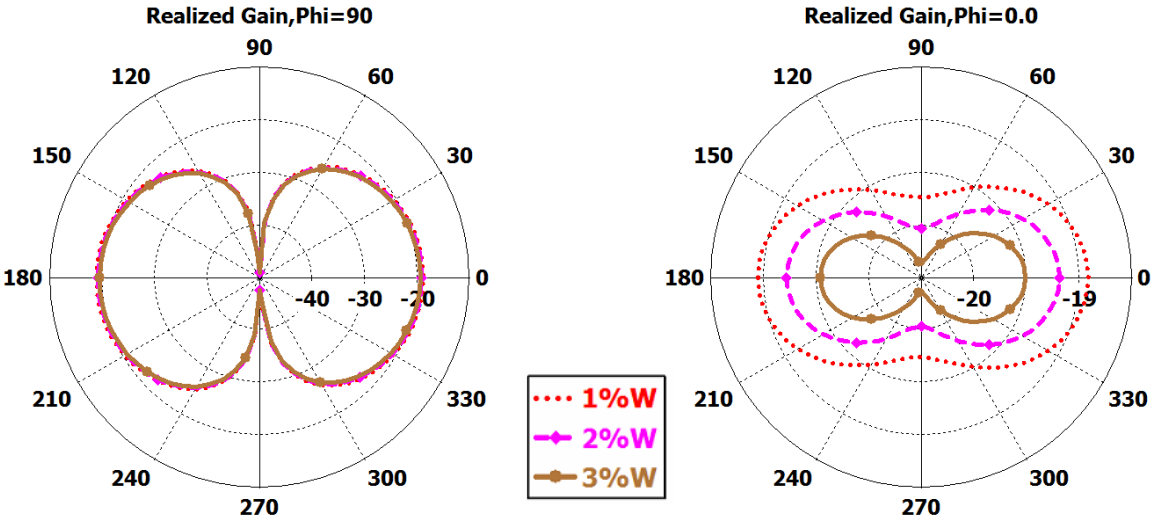

Figure 50: Realized gain of the antenna stretching in width, (a) E-plane, and, (b) H-plane.

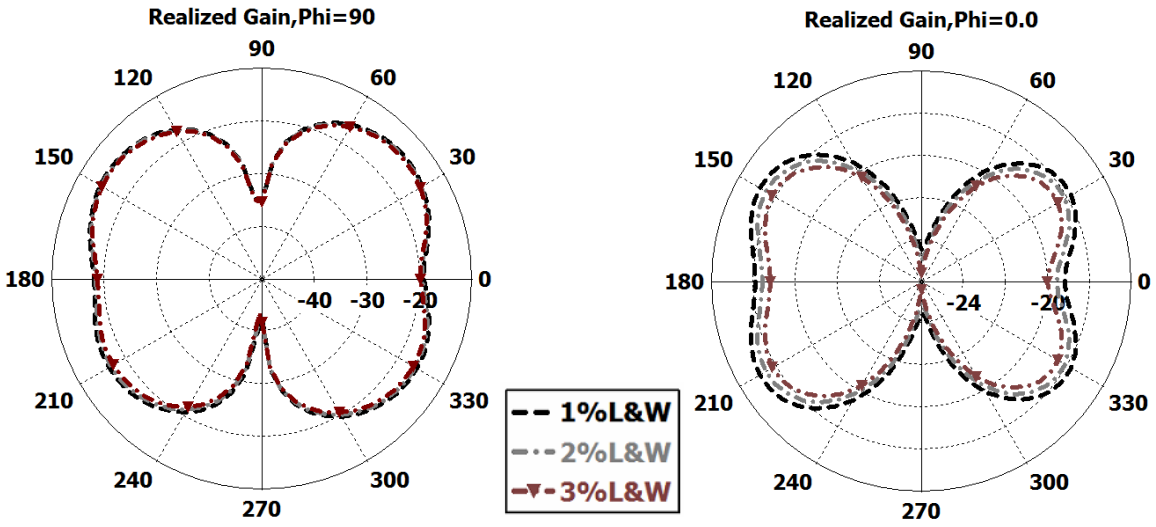

Figure 51: Realized gain of the antenna stretching in both length and width, (a) E-plane, and, (b) H-plane.

Table 7: Simulated S_{11} and gain at 5.8 GHz for monopole antenna under stretching conditions.

Parameter		f_r (GHz)	S_{11} (dB) @ 5.8 GHz	Gain (dBi) @ 5.8 GHz
Original	-	5.59	-30	1.17
Stretching length, L	1%	5.53	-28.24	0.62
	2%	5.47	-25.85	0.70
	3%	5.41	-23.97	0.78
Stretching width, W	1%		-0.125	-18.91
	2%		-0.119	-19.19
	3%		-0.112	-19.51
Stretching L and W	1%		-0.122	-19.20
	2%		-0.113	-19.58
	3%		-0.105	-20.01

4.3 Performance of the Stretched CPW Monopole Antenna on EBG

In this section we will discuss the antenna perfromance under different stretching condition on the EBG structure and compare it with the previous performance of the EBG antenna in free-space. Under the spacesuit pressure the textile substrate of the antenna tends to stretch while the flexible substrate of the EBG structure is less prone to stretch, In the simulation the EBG dimensions are kept original and only antenna dimesions are changed based on the percentage of the stretching. Again the antenna was stretched in length, width and both length and width togetehr from 1% to 3% of the original dimension. The antenna and EBG are integrated the same way it was done earlier. Figures 52-54 show the S-parameters of the antenna stretched in length, width and both in length and width, respectively.

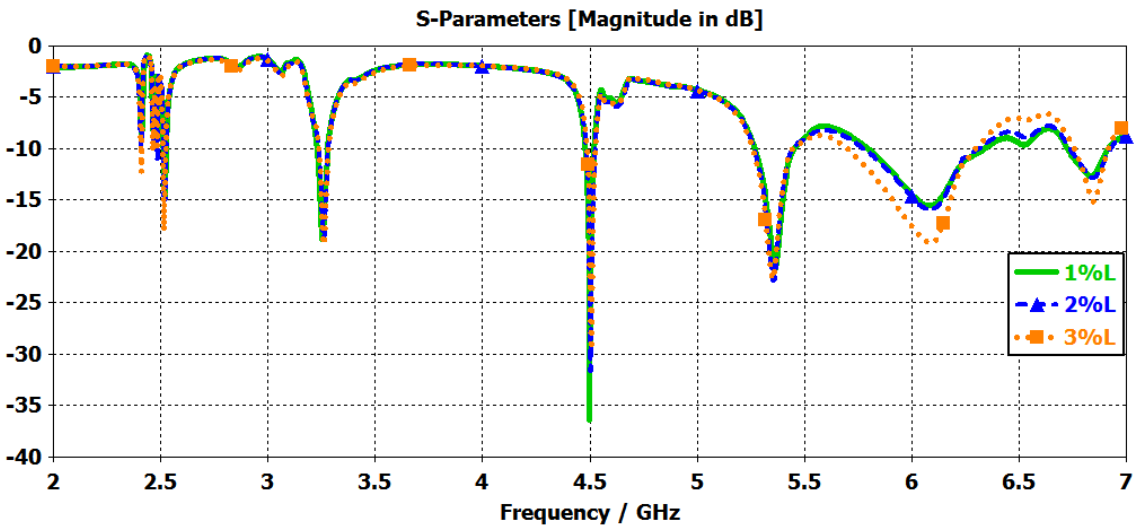

Figure 52: Reflection co-efficient of the antenna on EBG when stretched in length (L).

It can be seen from figure 52 that the resonannt frequency for length stretching is shifted to 4.5 GHz in comparison to original EBG antenna's 5.3 GHz. The S-parameter at

5.8 GHz for length stretching is around -10.3 dB , which is almost similar to the original's -10.59 dB.

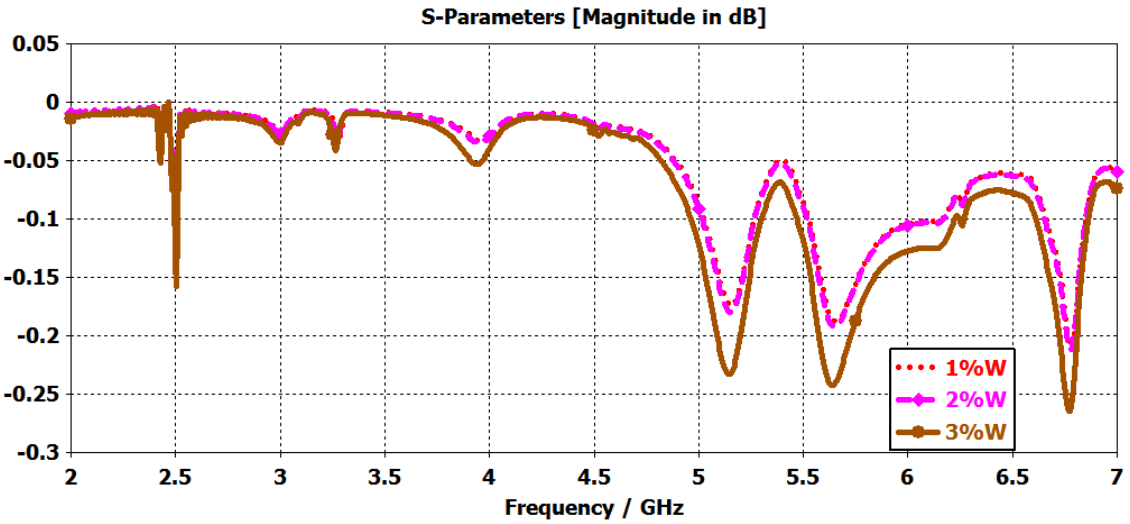

Figure 53: Reflection co-efficient of the antenna on EBG when stretched in width (W).

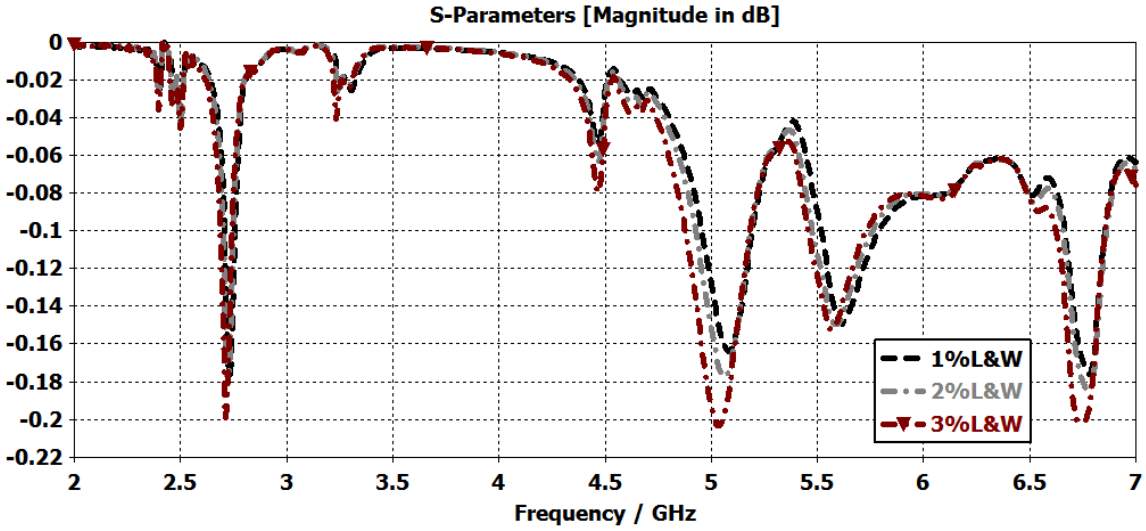

Figure 54: Reflection co-efficient of the antenna on EBG when stretched in both length and width (L&W).

From Figures 53 and 54 it can be noticed that when the antenna is stretched in width or both length and width together the perfromance of the antenna on EBG also drops drastically.

Figures 55-57 illustrate the realized gain patterns in the E-plane of the EBG antenna when stretched in length, width and in length and width togetehr. The gain when antenna was stretched in length alone is 8.37 dBi which is almost 1 dBi better than the orignal EBG antenna. On the other hand the when the antenna is stretched in width the E-plane gain is about -7.7 dBi. When stretched in both length and width the gain is -9.62 dBi. The antenna obviously is not working when it is streched in E-plane.

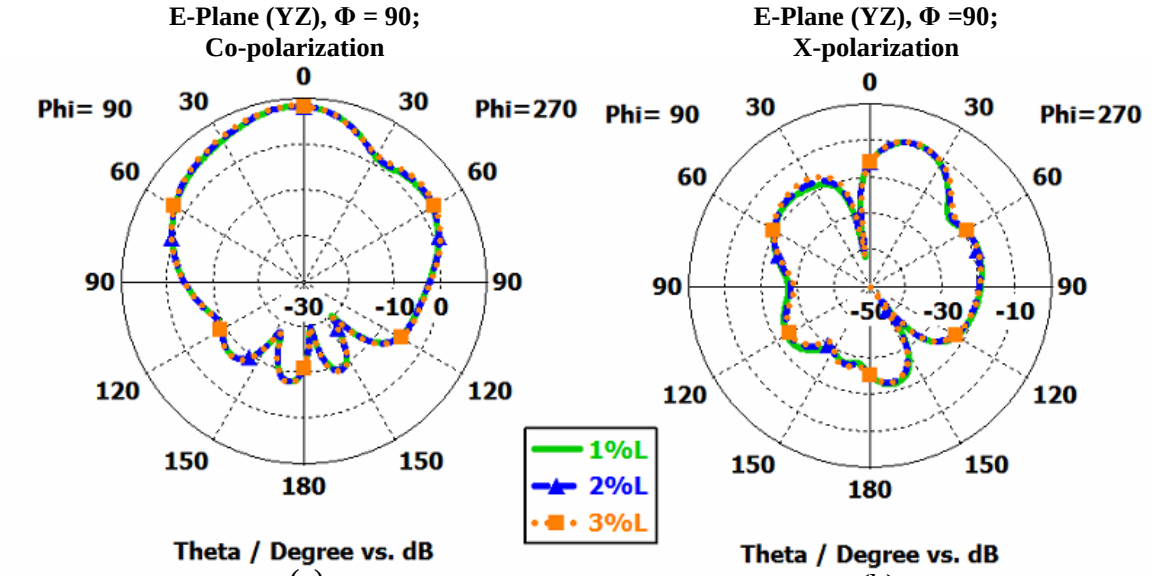

Figure 55: E-plane realized gain of EBG antenna stretched in length, (a) co-polarization, and, (b) cross-polarization.

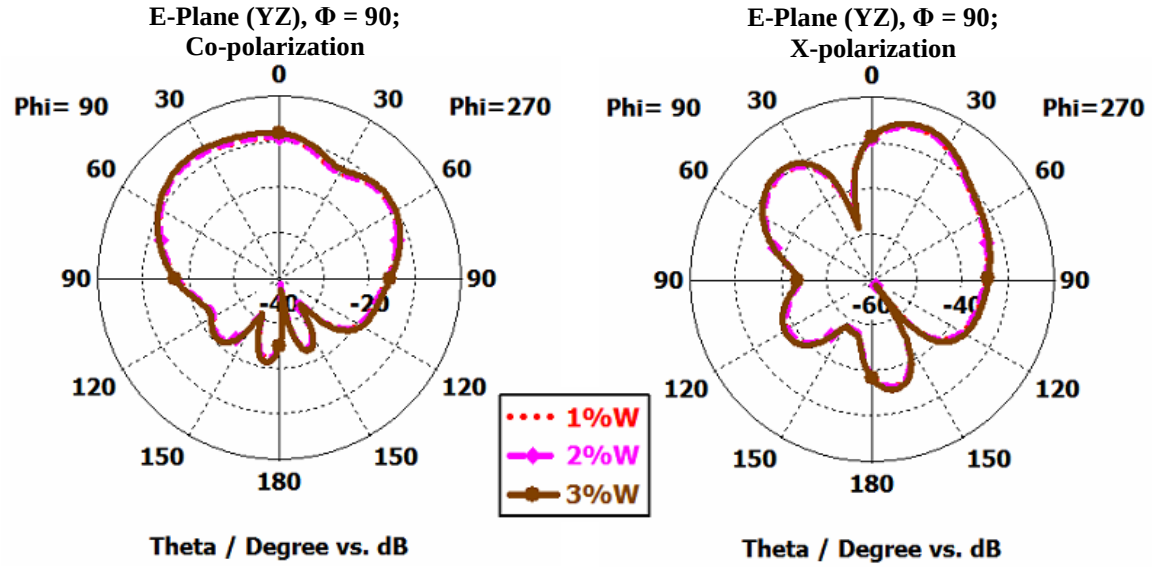

Figure 56: E-plane realized gain of EBG antenna stretched in width, (a) co-polarization, and, (b) cross-polarization.

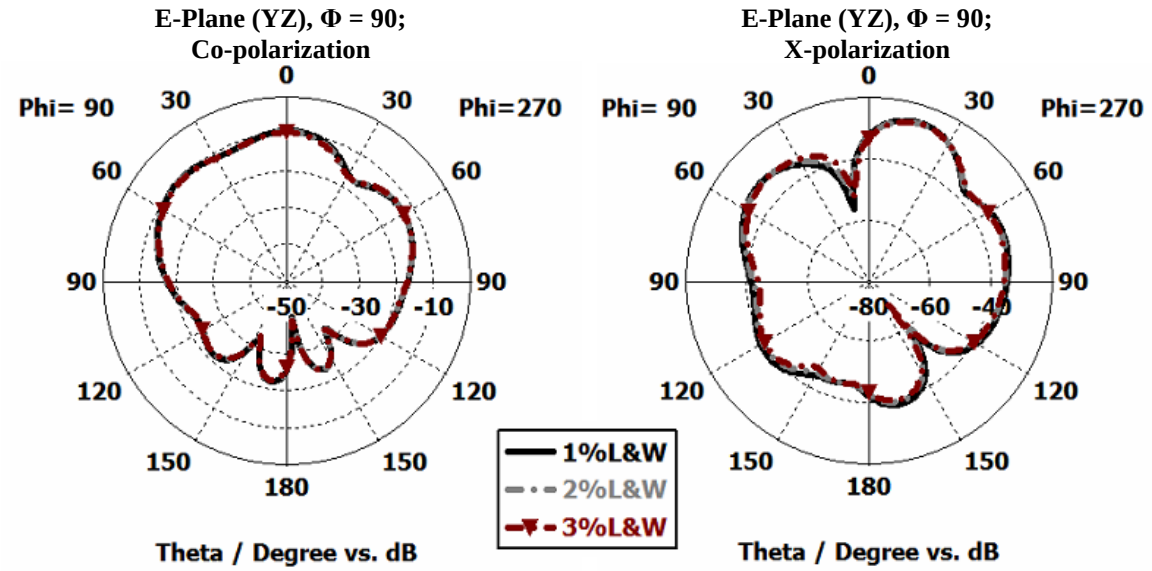

Figure 57: E-plane realized gain of EBG antenna stretched in length and width, (a) co-polarization, and, (b) cross-polarization.

Figures 58-60 show the H-plane gain patterns of the antenna on EBG. With stretching in eht length the gain is about 8.25 dBi. Stretching in width the gain reduces to -9.11 dBi, and when streched in both length and width gain is reduced to -9.61 dBi.

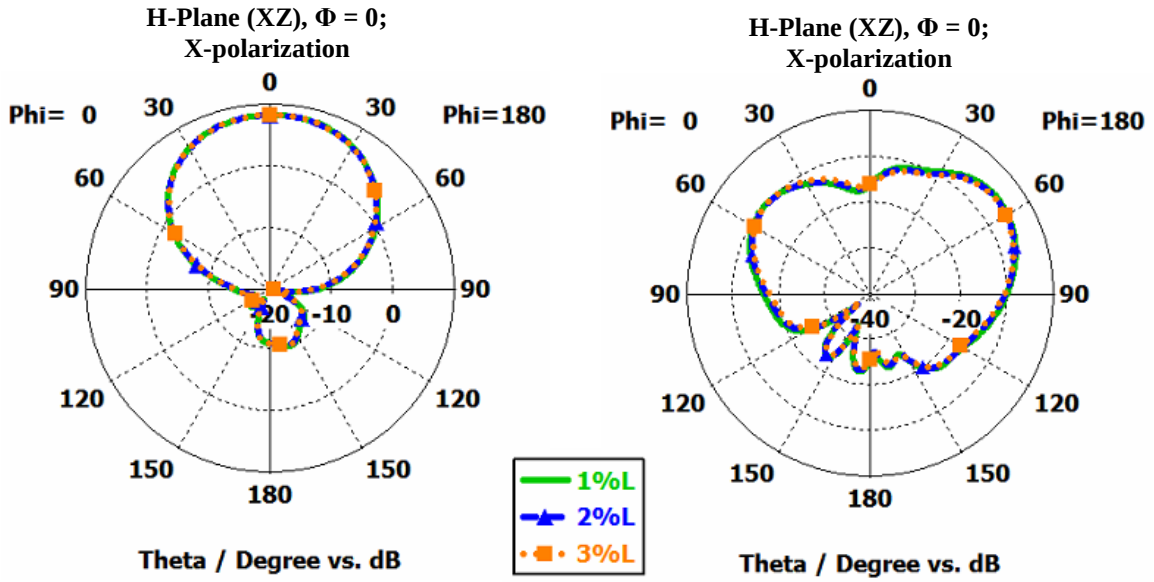

Figure 58: H-plane realized gain of EBG antenna stretched in length, (a) co-polarization, and, (b) cross-polarization.

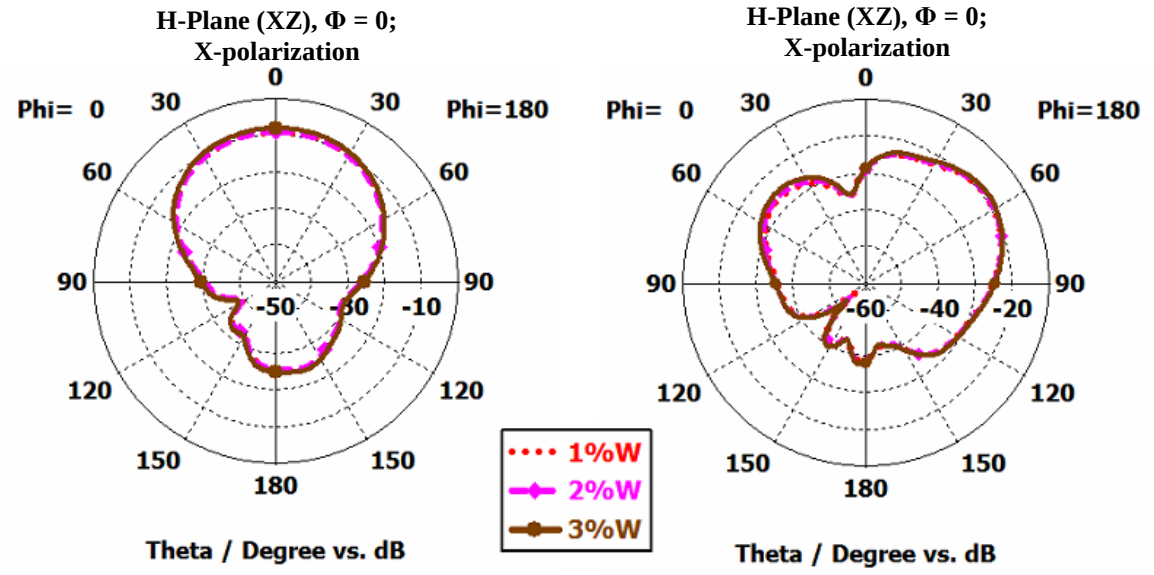

Figure 59: H-plane realized gain of EBG antenna stretched in width, (a) co-polarization, and, (b) cross-polarization.

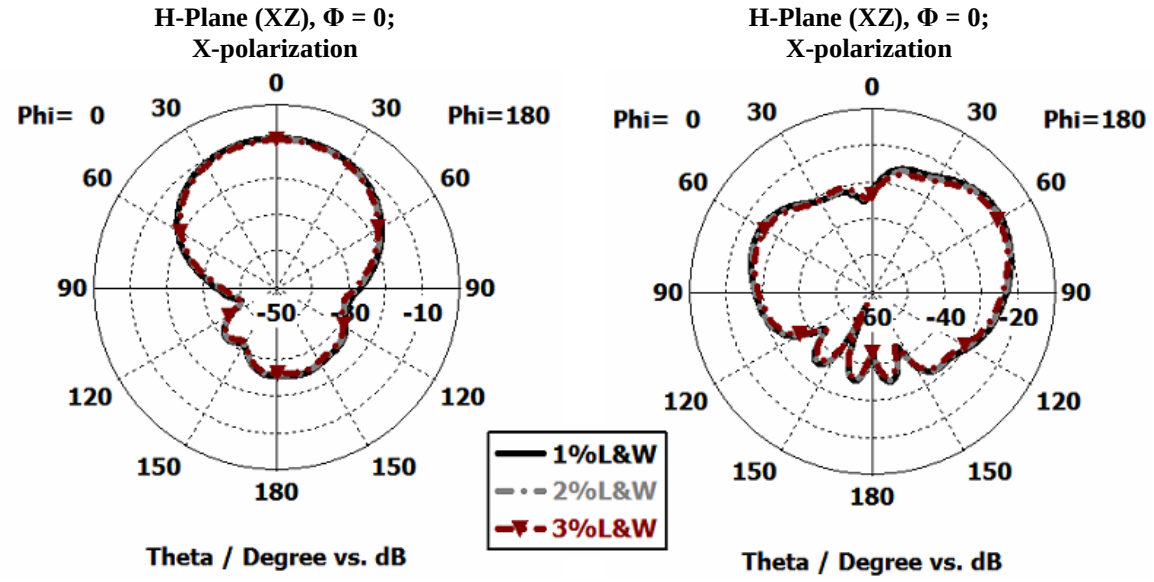

Figure 60: H-plane realized gain of EBG antenna stretched in length and width, (a) co-polarization, and, (b) cross-polarization.

Table 8: Simulated S_{11} and gain summary at 5.8 Ghz for antenna on EBG under different stretching effects.

Stretch		f_r (GHz)	S_{11} (dB) @ 5.8 GHz	Gain (dBi) @ 5.8 GHz	E-plane (copol-crosspol) (dB)	H-plane (copole-crosspol) (dB)
L	1%	5.33	-10.38	8.186	17.43	13.54
	2%	5.27	-11.48	8.180	17.42	13.85
	3%	5.25	-12.74	8.236	17.22	13.91
W	1%		-0.133	-9.191	17.67	10.29
	2%		-0.132	-9.110	17.81	10.37
	3%		-0.155	-8.115	17.82	10.77
L & W	1%		-0.110	-9.147	16.64	10.34
	2%		-0.120	-9.447	16.63	10.34
	3%		-0.130	-9.623	16.56	10.77

In Table 8 simulation results of the EBG antenna is summerized. Also the differences between the co-pol and cross-pol maximum levels (in dB) are given.

CHAPTER V

CONCLUSION AND FUTURE WORK

5.1 Introduction

The design and fabrication of fully textile wearable antennas integrated with EBG structures was studied in this thesis. The details of design cycle of wearable antennas including suitable material selection, EBG design, and integration of EBG with wearable antennas, performance of the EBG antenna on spacesuit material, performance of the antenna under stretching effects and finally, measurements of radiation performance of the overall antenna system were presented. It was shown that the performance of wearable antennas improves by EBG integration. In this chapter, summary of the main research work of the thesis, its significance and conclusions based on the results will be presented. To conclude, proposals for future work and continuation of the work will be presented.

5.2 Conclusions

The thesis has presented a wearable CPW-fed monopole antenna for 5.8 GHz ISM band and an EBG structure is used to enhance its performance. The EBG structure is an array of 3 × 2 unit cells and has dimensions of 122.2 × 94.8 mm^2. The antenna is intended to be used on human body (astronaut spacesuit) and back radiation of the antenna is a

concern. Therefore, EBG was added to the antenna. EBG does not allow the propagation of waves in all directions at a specific frequency band, and the structure, like a mirror, reflects back all electromagnetic waves. As a result, there will be less back radiation. The FBR is improved from 0.09 dB to 21.87 dB when EBG structure is used. In addition, the EBG structure improved the gain of the antenna by 6.11dB, from 1.17 dBi to 7.28 dBi.

The performance of the antenna, with and without EBG, was also investigated when placed on the spacesuit material. The spacesuit material has more significant effects when the antenna is not on the EBG structure. In this case, the impedance bandwidth decreases by 300 MHz compared to the antenna in free-space (7.3 GHz bandwidth) and the reflection co-efficient at 5.8 GHz is almost 5 dB less than the antenna in free-space. On the other hand, the EBG antenna with and without spacesuit material has reflection coefficient -10.59 dB and -12.59 dB, respectively. The impedance bandwidth is about 4.6 GHz at -8 dB for the EBG antenna on spacesuit, which is the same for the EBG antenna in free space at -10 dB.

Additionally, realized gain of the E-plane of the antenna on spacesuit shows about 0.5 dB increment (from 1.16 dB to 1.63 dB) and almost 3 dB (-98.4 dB to -95.1 dB) increment in the cross-polarization compared to the antenna in free-space. About 0.5 dB increment in co-polarization and 3 dB increment in cross-polarization of the H-plane was also seen. For the antenna integrated on EBG the realized gain was 7.28 dBi in free-space and 6.38 dBi, for the EBG antenna on spacesuit. The FBR of the EBG antenna on spacesuit is 17.75 dB, which is around 5 dB less than the EBG antenna in free-space (22.23 dB).

The antenna's textile material was considered to be stretched up to 3% due to pressure inside the spacesuit. It makes it important to evaluate the performance of the antenna under stretching conditions. The stretching is done in three different ways. Length only, width only, and length and width together. From the simulation results it was shown that when the antenna is stretched in length (E-plane) the performance remains close to the performance of the original antenna. However, the antenna may not be stretched in width, or length and width together, without degrading the antenna performance.

Although the EBG material is flexible, it is less prone to stretching. As a result simulation has been done by stretching the antenna only and keeping EBG in its original shape. The results are similar to the single antenna stretching. Stretching in length does not have pronounced effects on the antenna performance. On the other hand antenna's performance deteriorates if it is stretched in width or length and width together.

5.3 Future Work

This thesis has presented wearable antenna design cycle and proposed a new wearable antenna for spacesuit applications. However, any new design leads to more questions and future studies that needs further research. There is still an enormous amount of research and development that needs to be performed in this area.

Firstly, after considering different materials Pellon substrate was selected in this research. There is still need for study on material selection. There are a variety of textile materials available that need to be studied for their viability and suitability in wearable antenna designs. Also more attention needs to be paid to the firmness and durability of fabric in the final selection of materials.

Secondly, conventional soldering method was used to connect SMA connectors to the conducting fabric. The heat generated by the soldering machine can cause the conducting fabric to be burnt out. Also the soldered connection between metal connector and conducting fabric is brittle and tend to break easily if some force is applied. Rather than using conventional soldering method some new solder-less techniques can be proposed in future study to avoid this problem.

Thirdly, wearable antennas designed in this research are not tested under bending, crumbling and wet conditions. These topics can be explored in future studies. If performance deteriorates under wet conditions then search needs to be carried out on waterproof materials for future wearable communication designs.

Fourthly, stretching conditions have been investigated based on simulation results. However, measurements of the antenna under different stretching condition can be carried out as future experiment.

Lastly, the interaction between the proposed EBG wearable antenna and the human body is important. When the antenna is placed in very close proximity to the body, it requires investigations and finding methods to reduce the loading effects of human body. On body measurements are of interest and they are potentially important in order to further validate the antenna design for wearable antenna application.

REFERENCES

[1] L. Vallozzi, P. Van Torre, C. Hertleer, and H. Rogier, “A textile antenna for off-body communication integrated into protective clothing for firefighters,” *IEEE Trans Antennas Propag*., vol. 57, no. 4, pp. 919–925, Apr. 2009.

[2] E. K. Kaivanto, M. Berg, E. Salonen, and P. de Maagt, “Wearable circularly polarized antenna for personal satellite communication and navigation,” *IEEE Trans. Antennas Propag*., vol. 59, no. 12, pp. 4490–4496, Dec. 2011.

[3] P. Salonen and H.Hurme, “A novel fabric WLAN antenna for wearable applications,” *IEEE Trans Antennas Propagation (AP-S).*, vol. 2, pp. 700–703, Jun. 22–27, 2003.

[4] Dalia M.N. Elsheakh, Esmat A. Abdallah and Hala A. Elsadek, “Antenna Designs with Electromagnetic Band Gap Structures”. *INTECH Open Access Publisher*, 2012.

[5] J. Hu, “Overview of flexible electronics from ITRI’s viewpoint,” in *VLSI Test Symposium (VTS)* 28th, 2010, pp. 84.

[6] A. Nathan and B. R. Chalamala, “Special Issue on Flexible Electronics Technology, Part 1: Systems and Applications,” in *Proceedings of the IEEE, (7)*, 1993, pp. 1235-1238.

[7] M. A. R. Osman, M. K. Abd Rahim, M. Azfar Abdullah, N. A. Samsuri, F. Zubir, and K. Kamardin, "Design, implementation and performance of ultra-wideband textile antenna," *Progress In Electromagnetics Research B*, vol. 27, pp. 307-325, 2011.

[8] L. Josefsson and P. Persson, *Conformal array antenna theory and design*. Hoboken, NJ: Wiley-IEEE Press, 2006.

[9] S. Bashir, "Design and synthesis of non-uniform high impedance surface based wearable antennas," Ph.D. thesis, Loughborough University, 2009.

[10] Zhu, S.Z. and Langley, R., “Dual-band wearable textile antenna on an EBG substrate”. *IEEE Transactions on Antennas and Propagation*, 57 (4). pp. 926-935, 2009.

[11] A. Tsolis, W. G. Whittow, A. A. Alexandridis, and J. Y. C. Vardaxoglou, "Embroidery and Related Manufacturing Techniques for Wearable Antennas: Challenges and Opportunities," *Electronics*, vol. 3, pp. 314-338, 2014.

[12] I. Locher, M. Klemm, T. Kirstein and G. Troster, "Design and characterization of purely textile patch antennas," *IEEE Transactions on Advanced Packaging*, vol. 29, pp. 777-788, 2006.

[13] C. Hertleer, H. Rogier, L. Vallozzi and F. Declercq, "A Textile Antenna based on High-Performance Fabrics," *Antennas and Propagation, 2007. EuCAP 2007. The Second European Conference on*, pp. 1-5, 2007.

[14] P. Salonen, Y. Rahmat-Samii, H. Hurme and M. Kivikoski, "Dual-band wearable textile antenna," in *IEEE Antennas and Propagation Society Symposium 2004 Digest Held in Conjunction with: USNC/URSI National Radio Science Meeting*, 2004, pp. 463-466.

[15] R. Langley and Shaozhen Zhu, "Dual band wearable antenna," *Antennas and Propagation Conference, 2008. LAPC 2008. Loughborough*, pp. 14-17, 2008.

[16] Yuehui Ouyang and W. Chappell, "Distributed Body-worn Transceiver System with the Use of Electro-textile Antennas," *Microwave Symposium, 2007. IEEE/MTT-S International*, pp. 1229-1232, 2007.

[17] Federal Communication Commission. Http://www.fcc.gov/oet/rfsafety/dielectric.html

[18] P. Salonen, L. Sydanheimo, M. Keskilammi and M. Kivikoski, "A small planar inverted-F antenna for wearable applications," in *Wearable Computers, 1999. Digest of Papers. the Third International Symposium on*, 1999, pp. 95-100.

[19] P. J. Massey, "Mobile phone fabric antennas integrated within clothing," in Antennas and Propagation, 2001.*Eleventh International Conference on (IEE Conf.Publ.no.480)*, 2001, pp. 344-347 vol.1.

[20] P. Salonen and L. Sydanheimo, "Development of an S-band flexible antenna for smart clothing," *in 2002 IEEE Antennas and Propagation Society International Symposium*, 2002, pp. 6-9.

[21] M. Tanaka and J. Jang, "Wearable microstrip antenna," in *2003 IEEE International Antennas and Propagation Symposium and USNC/CNC/URSI North American Radio Science Meeting*, 2003, pp. 704-707.

[22] A. Jafargholi, "VHF-LB Vest Antenna Design," *Antenna Technology: Small and Smart Antennas Metamaterials and Applications, 2007. IWAT '07. International Workshop on*, pp. 247-250, 2007.

[23] C. Cibin, P. Leuchtmann, M. Gimersky, R. Vahldieck and S. Moscibroda, "A flexible wearable antenna," *in Antennas and Propagation Society International Symposium, 2004.IEEE*, 2004, pp. 3589-3592 Vol.4.

[24] J. Slade, J. Teverovsky, B. Farrell, J. Bowman, M. Agpaoa-Kraus and P. Wilson, "Textile based antennas," in *Electronics on Unconventonal Substrates--Electrotextiles and Giant-Area Flexible Circuitse*, 2003, pp. 91-97.

[25] C. Cibin, P. Leuchtmann, M. Gimersky and R. Vahldieck, "Modified E-shaped PIFA antenna for wearable systems," in *URSl Intemational Symposium an Electromagnetic Theory*, 2004.

[26] B. Sanz-Izquierdo, F. Huang, J. C. Batchelor and M. Sobhy, "Compact antenna for WLAN on body applications," in *Microwave Conference, 2006.36th European*, 2006, pp. 815-818.

[27] B. Sanz-Izquierdo, F. Huang and J. C. Batchelor, "Covert dual-band wearable button antenna," *Electronic Letter*, vol. 42, pp. 668-670, 2006.

[28] B. Sanz-Izquierdo and J. C. Batchelor, "Wlan Jacket Mounted Antenna," *Antenna Technology: Small and Smart Antennas Metamaterials and Applications, 2007. IWAT '07. International Workshop on*, pp. 57-60, 2007.

[29] Y. Ouyang and W. Chappell, "Measurement of electrotextiles for high frequency applications," *Microwave Symposium Digest, 2005 IEEE MTT-S International*, pp. 4 pp., 2005.

[30] D. Cottet, J. Grzyb, T. Kirstein and G. Troster, "Electrical characterization of textile transmission lines," *Advanced Packaging, IEEE Transactions on*, vol. 26, pp. 182-190, 2003.

[31] Y. Ouyang and W. J. Chappell, "High Frequency Properties of Electro-Textiles for Wearable Antenna Applications," *Antennas and Propagation, IEEE Transactions on*, vol. 56, pp. 381-389, 2008.

[32] P. Salonen, Y. Rahmat-Samii, M. Schaffrath and M. Kivikoski, "Effect of textile materials on wearable antenna performance: A case study of GPS antennas," *in Antennas and Propagation Society International Symposium, 2004.IEEE*, 2004, pp. 459-462 Vol.1.

[33] P. Salonen, Y. Rahmat-Samii and M. Kivikoski, "Wearable antennas in the vicinity of human body," in *IEEE Antennas and Propagation Society Symposium 2004 Digest Held in Conjunction with: USNC/URSI National Radio Science Meeting*, 2004, pp. 467-470.

[34] M. Klemm, I. Locher and G. Troster, "A novel circularly polarized textile antenna for wearable applications*," in Conference Proceedings- 34th European Microwave Conference*, 2004, pp. 137-140.

[35] A. Tronquo, H. Rogier, C. Hertleer and L. Van Langenhove, "Robust planar textile antenna for wireless body LANs operating in 2.45 GHz ISM band," *Electronic Letter*, vol. 42, pp. 21-22, 2006.

[36] P. Salonen, J. Kim and Y. Rahmat-Samii, "Dual-band E-shaped patch wearable textile antenna," *in Antennas and Propagation Society International Symposium, 2005 IEEE*, 2005, pp. 466-469 Vol. 1A.

[37] C. Hertleer, H. Rogier and L. Van Langenhove, "A textile antenna for protective clothing," *Antennas and Propagation for Body-Centric Wireless Communications, 2007 IET Seminar on*, pp. 44-46, 2007.

[38] A. Galehdar and D. V. Thiel, "Flexible, light-weight antenna at 2.4GHz for athlete clothing," *Antennas and Propagation Society International Symposium, 2007 IEEE*, pp. 4160-4163, 2007.

[39] J. G. Santas, A. Alomainy and Yang Hao, "Textile Antennas for On-Body Communications: Techniques and Properties," *Antennas and Propagation, 2007. EuCAP 2007. the Second European Conference on*, pp. 1-4, 2007.

[40] T. F. Kennedy, P. W. Fink, A. W. Chu, N. J. Champagne, G. Y. Lin, and M. A. Khayat, "Body-worn E-textile antennas: the good, the low-mass, and the conformal," *IEEE Trans. Antennas Propag.*, vol. 57, no. 4, pp. 910-918, Apr. 2009.

[41] I. Oppermann, UWB: *Theory and Applications*. WileyBlackwell, 2004, pp. 248.

[42] M. Klemm and G. Troester, "Textile UWB Antennas for Wireless Body Area Networks," *Antennas and Propagation, IEEE Transactions on*, vol. 54, pp. 3192-3197, 2006.

[43] B. Sanz-Izquierdo, J. C. Batchelor and M. Sobhy, "UWB wearable button antenna," in *European Conference on Antennas and Propagation: EuCAP 2006*, 2006, pp. 4.

[44] B. Sanz-Izquierdo, J. C. Batchelor and M. I. Sobhy, "Compact UWB wearable antenna," in *LAPC 2007: 3rd Loughborough Antennas and Propagation Conference,* 2007, pp. 121-124.

[45] D. Sievenpiper, Lijun Zhang, R. F. J. Broas, N. G. Alexopolous and E. Yablonovitch, "High-impedance electromagnetic surfaces with a forbidden frequency band," *Microwave Theory and Techniques, IEEE Transactions on,* vol. 47, pp. 2059-2074, 1999.

[46] Fan Yang and Y. Rahmat-Samii, "Curl antennas over electromagnetic band-gap surface: a low profiled design for CP applications," *Antennas and Propagation Society International Symposium, 2001. IEEE,* vol. 3, pp. 372-375 vol.3, 2001.

[47] Fan Yang and Y. Rahmat-Samii, "Reflection phase characterization of an electromagnetic band-gap (EBG) surface," *Antennas and Propagation Society International Symposium, 2002. IEEE,* vol. 3, pp. 744-747, 2002.

[48] Fan Yang and Y. Rahmat-Samii, "Applications of electromagnetic band-gap (EBG) structures in microwave antenna designs," *Microwave and Millimeter Wave Technology, 2002. Proceedings. ICMMT 2002. 2002 3rd International Conference on,* pp. 528-531, 2002.

[49] P. Salonen, M. Keskilammi and L. Sydanheimo, "A low-cost 2.45 GHz photonic band-gap patch antenna for wearable systems," *Antennas and Propagation, 2001. Eleventh International Conference on (IEE Conf. Publ. no. 480),* vol. 2, pp. 719-723 vol.2, 2001.

[50] H. R. Raad, A. I. Abbosh, H. M. Al-Rizzo, and D. G. Rucker, "Flexible and compact AMC based antenna for telemedicine applications," *IEEE Trans. Antennas Propag.,* vol. 61, no. 2, pp. 524-531, Feb. 2013.

[51] P. Salonen, F. Yang, Y. Rahmat-Samii, and M. Kivikoski, "WEBGA-wearable electromagnetic band-gap antenna," in *Pro. IEEE AP-S Int. Symp.*, Monterey, CA, Jun. 2004, pp. 451-454.

[52] P. Salonen, F. Yang, Y. Rahmat-Samii and M. Kivikoski, "WEBGA - wearable electromagnetic band-gap antenna," *in IEEE Antennas and Propagation Society Symposium 2004 Digest Held in Conjunction with: USNC/URSI National Radio Science Meeting*, 2004, pp. 451-454.

[53] P. Salonen and Y. Rahmat-Samii, "Textile Antennas: Effects of Antenna Bending on Input Matching and Impedance Bandwidth," *Aerospace and Electronic Systems Magazine, IEEE,* vol. 22, pp. 18-22, 2007.

[54] Shaozhen Zhu, Luyi Liu and R. Langley, "Dual Band Body Worn Antenna," *Antennas and Propagation Conference, 2007. LAPC 2007.* Loughborough, pp. 137-140, 2007.

[55] S. Zhu and R. Langley, "Dual-band wearable antennas over EBG substrate," *Electronics Letters,* vol. 43, pp. 141-142, 2007. 2007.

[56] A. Alu, M. G. Silveirinha, A. Salandrino, and N. Engheta, "Epsilon-Near-Zero Metamaterials and Electromagnetic Sources: Tailoring the Radiation Phase Pattern," *Physical Review B,* vol. 75, no. 15, 2007.

[57] Y. Ning, C. Zhining, W. Yunyi and C. M. Y. W, " A novel two-layer compact electromagnetic bandgap (EBG) structure and its applications in microwave circuits", *Science in China (Series E),* Vol. 46, no. 4 August 2003.

[58] X. Q. Chen, X. W. Shi, Y. C. Guo, and C. M. Xiao, " A novel dual band transmitter using microstrip defected ground structure", *Progress In Electromagnetics Research, PIER 83,* pp. 1–11, 2008.

[59] C. S. Kim, J. S. Park, D. Ahn, and J. B. Lim, "A novel 1-D periodic defected ground structure for planar circuits," *IEEE Microwave Guided Wave Lett.,* vol. 10, pp. 131–133, Apr. 2000.

[60] M. Fallah-Rad and L. Shafai, "Enhanced performance of a microstrip patch antenna using high impedance EBG structure," *IEEE APS Int. Symp. Dig.,* vol. 3, pp. 982–5, June 2003.

[61] C. C. Chiau, X. Chen, and C. G. Parini, "A microstrip patch antenna on the embedded multi-period EBG structure," *Proceeding of the 6th Int. Symp. Antennas, Propagation and EM Theory,* pp. 96–106, 2003.

[62] H. Mosallaei and Y. Rahmat-Samii, "Periodic bandgap and effective dielectric materials in electromagnetics: characterization and applications in nanocavities and waveguides," *IEEE Trans. Antennas and Propag.,* vol. 51, pp. 549–63, April 2003.

[63] F. Yang and Y. Rahmat-Samii, "Bent monopole antennas on EBG ground plane with reconfigurable radiation patterns," *2004 IEEE APS Int. Symp. Dig.,* Vol. 2, pp. 1819–1822, Monterey, CA, June 20–26, 2004.

[64] E. Yablonovitch, "Inhibited Spontaneous Emission in Solid-State Physics and Electronics," *Physical Review Letters,* vol. 58, no. 20, pp. 2059-2062, 1987.

[65] W. Barnes, T. Priest, S. Kitson, J. Sambles, "Photonic Surfaces for Surface-Plasmon Polaritons", *Phys. Rev. B,* vol. 54, pp. 6227, 1996.

[66] F. Yang, and Y. Rahmat-Samii, "Reflection Phase Characterizations of the EBG Ground Plane for Low Profile Wire Antenna Applications," *IEEE Trans. on Antennas Propag.,* vol. 51, no. 10, Oct. 2003.

[67] J. R. Sohn, H. S. Tae, J. G. Lee, and J. H. Lee, "Comparative Analysis of Four Types of High Impedance Surfaces for Low Profile Antenna Applications," *Ant. And Propagat. Society International Symposium,* vol. 1A, pp. 758 - 761, 2005.

[68] S. F. Mahmoud, "A New Miniaturized Annular Ring Patch Resonator Partially Loaded by A Metamaterial Ring with Negative Permeability and Permittivity," *IEEE Antennas and Wireless Propagation Letters,* vol. 3, pp. 19 - 22, 2004.

[69] J. R. Sohn, H. S. Tae, J. G. Lee, and J. H. Lee, "Comparative Analysis of Four Types of High Impedance Surfaces for Low Profile Antenna Applications," *Ant. And Propagat. Society International Symposium*, vol. 1A, pp. 758 - 761, 2005.

[70] C. A. Balanis, *Advanced Engineering Electromagnetics.* New York; London: Wiley, 1989.

[71] C. A. Balanis, *Antenna Theory: Analysis and Design*. , 3rd ed. Hoboken, NJ: John Wiley, 2005, pp. 1117.

[72] D. Sievenpiper, "High Impedance Electromagnetic Surfaces," *PhD Dissertation at University of California, Los Angeles,* 1999.

[73] R. E. Collin and IEEE Antennas and Propagation Society, *Field Theory of Guided Waves*. , 2nd ed. New York: IEEE Press, 1991, pp. 851.

[74] D. Sievenpiper, L. Zhang and E. Yablonovitch, "High-impedance electromagnetic ground planes," *Microwave Symposium Digest, 1999 IEEE MTT-S International*, vol. 4, pp. 1529-1532 vol.4, 1999.

[75] Fan Yang and Y. Rahmat-Samii, "Microstrip antennas integrated with electromagnetic band-gap (EBG) structures: a low mutual coupling design for array applications," *Antennas and Propagation, IEEE Transactions on*, vol. 51, pp. 2936-2946, 2003.

[76] D. Pozar and D. Schaubert, "Scan blindness in infinite phased arrays of printed dipoles," *Antennas and Propagation, IEEE Transactions on*, vol. 32, pp. 602-610, 1984.

[77] Q. Li, A. Feresidis, M. Mavridou, and P. Hall, "Miniaturized double-layer EBG structures for broadband mutual coupling reduction between UWB monopoles," *IEEE Trans. Antennas Propag.*, vol. 63, no. 3, pp. 1168-1171, Mar. 2015.

[78] R. Coccioli, F.-R. Yang, K.-P. Ma, and T. Itoh, "Aperture-coupled patch antenna on UC-PBG substrate," *IEEE Trans. Microwave Theory Tech.*, vol. 47, pp. 2123-2130, Nov. 1999.

[79] F. Yang, A. Aminian, and Y. Rahmat-Samii, "A novel surface-wave antenna design using a thin periodically loaded ground plane," *Microw. Opt. Technol. Lett.*, vol. 47, pp. 240-245, Nov. 2005.

[80] G. Goussetis, A. P. Feresidis, and J. C. Vardaxoglou, "Tailoring the AMC and EBG characteristics of periodic metallic arrays printed on grounded dielectric substrate," *IEEE Trans. Antennas Propag.*, vol. 54, no. 1, pp. 82-89, 2006.

[81] F. Yang and Y. Rahmat-Samii, "Mutual coupling reduction of microstrip antennas using electromagnetic band-gap structure," *Proc IEEE AP-S Dig. 2*, pp. 478–481, 2001.

[82] *CST Microwave Studio*, visited December 2013.

[83] J. R. Sohn, H. S. Tae, J.-G. Lee, and J.-H. Lee, "Comparative analysis of four types of high-impedance surfaces for low profile antenna applications," in *Proc. IEEE AP-S Int. Symp. (Digest) Antennas Propag. Society*, 2005, pp. 758-761.

[84] P. de León, G. L. Harris, and A. M. Wargetz "Design, construction, and implementation of an inflatable lunar habitat base with pressurized rover and suit ports," *43rd International Conference on Environmental Systems*, Vail, Colorado. 14-18 July 2013.